

UNCLASSIFIED

---

AD 267 570

*Reproduced  
by the*

ARMED SERVICES TECHNICAL INFORMATION AGENCY  
ARLINGTON HALL STATION  
ARLINGTON 12, VIRGINIA



---

UNCLASSIFIED

NOTICE: When government or other drawings, specifications or other data are used for any purpose other than in connection with a definitely related government procurement operation, the U. S. Government thereby incurs no responsibility, nor any obligation whatsoever; and the fact that the Government may have formulated, furnished, or in any way supplied the said drawings, specifications, or other data is not to be regarded by implication or otherwise as in any manner licensing the holder or any other person or corporation, or conveying any rights or permission to manufacture, use or sell any patented invention that may in any way be related thereto.

AIR FORCE  
BALLISTIC MISSILE DIVISION  
TECHNICAL LIBRARY

Document No. \_\_\_\_\_

Copy No. \_\_\_\_\_

267 570

AERONAUTRONIC SYSTEMS, INC.

A SUBSIDIARY OF

REG NO. \_\_\_\_\_  
LOG NO. 8-8309  
WDSOT. \_\_\_\_\_

8-4953  
64.2

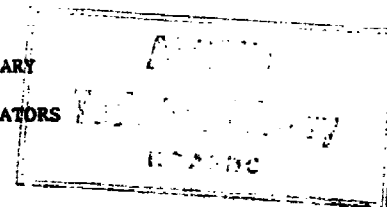
AERONUTRONIC SYSTEMS, INC.  
a Subsidiary of  
FORD MOTOR COMPANY  
1234 Air Way, Glendale, California

Publication No. U-166  
March 19, 1958

**NOTE:** Do not return  
to **WDSOT** Destroy  
according to applicable  
security regulations

REPORT CONCERNING

COMBUSTION IN THE TURBULENT BOUNDARY  
LAYER OF CHEMICALLY ACTIVE SUBLIMATORS



M. R. Denison

Submitted to:

BALLISTIC MISSILE DIVISION  
AIR RESEARCH AND DEVELOPMENT COMMAND  
Inglewood, California

## SUMMARY

An aerothermochemical analysis of chemically active surfaces immersed in a high speed stream of an oxidizing gas mixture is presented. The analysis applies to turbulent flow over blunt bodies whose surface material passes into the gaseous phase without going through the liquid state. This report is a sequel to the previous investigation<sup>(1)</sup> of laminar flow under the same environmental conditions. The theory is developed in general for a whole class of sublimators and is then applied to the particular case of graphite combustion about which a great deal of fundamental data is available.

## ACKNOWLEDGMENTS

The author wishes to express his appreciation to Professor F. E. Marble of California Institute of Technology, a consultant to Aeronutronic Systems, Inc., as well as Dr. D. Altman and Dr. D. A. Dooley of Aeronutronic Systems, Inc. for many valuable discussions. In addition, he wishes to thank Mr. L. Sashkin for programming the analytical results for the IBM 650 computer.

Note: The analysis presented in this publication was initiated under the sponsorship of Aeronutronic Systems, Inc. and completed under Air Force contract No. AF04(647)-155.

# TABLE OF CONTENTS

<u>SECTION</u>		<u>PAGE</u>
1	INTRODUCTION	1
2	TURBULENT BOUNDARY LAYER EQUATIONS	3
3	CHEMICAL REACTIONS, MASS TRANSFER, AND HEAT TRANSFER	9
	3.1 Interaction of Diffusion and Chemical Reactions.....	9
	3.2 Chemical Model.....	10
	3.3 Mass Transfer at Surface.....	11
	3.4 Atomic Mass Fractions at Surface.....	14
	3.5 Heat Transfer.....	15
4	ESTIMATION OF TURBULENT SKIN FRICTION	17
	4.1 Velocity Distribution.....	17
	4.2 Solution of Momentum Integral for Skin Friction.....	20
	4.3 Effect of Chemical Structure of Boundary Layer on Integral $\phi$ .....	24
5	COMBUSTION OF GRAPHITE	28
	5.1 Chemical Considerations.....	28
	5.2 General Surface Mass and Heat Transfer.....	29
	5.3 Evaluation of the Integral $\phi$ for Graphite in Air.....	31
	5.4 Inviscid Flow Field for Blunt Bodies.....	34
	5.5 Heat and Mass Transfer Distributions on a Hemisphere.....	36
	LIST OF REFERENCES	39

APPENDIX

	<u>PAGE</u>
A      TURBULENT CONSERVATION EQUATIONS FOR REACTING GAS MIXTURES	41
B      DISCUSSION OF THE NUMBER OF INDEPENDENT RELATIONS FOR MOLECULAR SPECIES	48
C      ESTIMATION OF COMBUSTION ZONE THICKNESS	51

# LIST OF FIGURES

<u>FIGURE</u>		<u>PAGE</u>
1	Effect of Flow Parameter, Accommodation Coefficient, and Temperature on B.....	53
2	Effect of Flow Parameter Accommodation Coefficient, and Temperature on $\alpha_w$ .....	54
3	Effect of Flow Parameter, Accommodation Coefficient and Temperature on Enthalpy Potential.....	55
4	Effect of Flow Parameter, Accommodation Coefficient and Temperature on Surface Mass Loss.....	56
5	Effect of Pressure and Temperature on B.....	57
6	Effect of Pressure and Temperature on $\alpha_w$ .....	58
7	Effect of Pressure and Temperature on Enthalpy Potential.....	59
8	Universal Plot for Integrand of $\phi$ (Graphite in Air).....	60
9	Variation of $\gamma_e$ with Mach Number, Altitude and Angular Location on a Hemisphere.....	61
10	Effective Reynolds Number Parameter for a Hemisphere.....	62
11	Heat Flux Distribution on Hemisphere-- 100,000 ft Altitude.....	63
12	Mass Flux Distribution on Hemisphere-- 100,000 ft Altitude.....	64
13	Distribution of Parameter B on Hemisphere-- 100,000 ft Altitude.....	65
14	Distribution of Parameter $\alpha_w$ on Hemisphere-- 100,000 ft Altitude.....	66



<u>FIGURE</u>		<u>PAGE</u>
15	Heat Flux Distribution on Hemisphere-- 50,000 ft Altitude.....	67
16	Mass Flux Distribution on Hemisphere-- 50,000 ft Altitude.....	68
17	Distribution of Parameter B on Hemisphere-- 50,000 ft Altitude.....	69
18	Distribution of Parameter $\phi_w$ on Hemisphere-- 50,000 ft Altitude.....	70
19	Distribution of Integral $\phi$ on Hemisphere.....	71

## NOMENCLATURE

### SYMBOLS

$a$	skin friction parameter, see equation (42)
$B$	ratio of mass injection to skin friction, see equation (31)
$B^*$	value of $B$ with reactants in stoichiometric proportion, see equation (34)
$C_{fe}$	skin friction coefficient based on local free stream conditions
$C_p$	specific heat of mixture
$D$	molecular diffusion coefficient
$D_T$	turbulent diffusion coefficient, see equation (10)
$\bar{\epsilon}$	rate of strain tensor
$f$	fuel species
$h$	enthalpy of mixture
$h_{ew}$	enthalpy of air at wall conditions, see equation (37)
$h_{fs}$	enthalpy of fuel in solid state
$h_i$	enthalpy of chemical species $i$ including heat of formation
$h_i^o$	heat of formation of $i$ th chemical species
$h_s$	total enthalpy of mixture
$h_{se}$	local free stream total enthalpy
$H$	enthalpy of mixture with zero datum, see equation (66)
$K$	thermal conductivity
$K_i$	mass fraction of $i$ th species
$K_{pe}$	equilibrium constant based on pressure for reaction $i$

$l$	mixing length
$Le_r$	turbulent Lewis number, see equation (12)
$\dot{m}_{i,w}$	net mass flux of $i$ th species at the surface
$\dot{m}_{i,0}$	flux of species $i$ striking surface
$\dot{m}_{i,f}$	flux of species $i$ outward from surface
$\dot{m}_w$	net mass flux of mixture at surface
$M$	molecular weight of mixture
$M_i$	molecular weight of $i$ th species
$M_1$	free stream Mach number
$N$	atomic nitrogen
$O$	atomic oxygen
$P$	pressure
$\vec{P}$	stress tensor
$P_i$	partial pressure of $i$ th species
$P_1$	free stream pressure
$P_1$	first product species
$P_2$	second product species
$P_{t2}$	stagnation pressure behind bow shock
$Pr_r$	turbulent Prandtl number, see equation (11)
$\vec{q}$	mass average velocity vector
$q_a$	heat absorbed by conduction into the body and/or radiation away from the surface
$\vec{q}_{di}$	diffusion velocity vector

$\vec{Q}$	flux of heat by diffusion and conduction
$Q_{row}$	heat of combustion at wall conditions
$r_0$	distance from axis of symmetry to body surface
$\bar{r}_{mi}$	ratio of mass of atomic species $m$ to unit mass of chemical species $i$
$\tilde{Re}_w$	effective Reynolds number for blunt bodies, see equation (51)
$Re_\infty$	free stream Reynolds number based on body radius
$R_0$	universal gas constant
$S$	entropy
$t$	time
$T$	temperature
$T_w$	wall temperature
$u$	component of velocity in $x$ direction
$u_e$	local free stream value of $u$
$v$	component of velocity in $y$ direction
$w_i$	rate of production of $i$ th chemical species
$x$	tangential distance from stagnation point along body surface
$y$	distance normal to body surface
$z$	velocity ratio $u/u_e$
$\alpha$	exponent used to trace influence of shear distribution
$\alpha_{mi}$	number of atoms of atomic species $m$ per molecule of molecular species $i$

$\alpha_w$	fraction of heat of combustion which increases enthalpy potential, see equation (37)
$\beta$	exponent used to trace influence of mixing length assumption
$\gamma_e$	polytropic exponent, see equation (70)
$\gamma_1$	free stream ratio of specific heats
$\bar{T}_m$	atomic mass fraction, see equation (4)
$\bar{T}_{O_2}$	atomic mass fraction for oxygen at outer edge of boundary layer
$\delta$	boundary layer thickness
$\epsilon$	eddy viscosity, see equation (8)
$\epsilon_i$	degree of dissociation of $i$ th species
$\theta$	angular distance from stagnation point
$\kappa$	body curvature
$\kappa_T$	eddy thermal conductivity, see equation (9)
$\lambda_{fw}$	heat of sublimation at surface conditions
$\mu$	viscosity
$\nu_i$	stoichiometric coefficient of $i$ th species
$\nu_w$	kinematic viscosity at surface conditions
$\xi$	parameter for determining atomic mass fractions, see equation (53)
$\rho$	density of mixture
$\rho_e$	density at outer edge of boundary layer
$\sigma_i$	accommodation coefficient for $i$ th species
$\tau$	shear stress

$\tau_w$	wall shear stress
$\phi$	integral defined by equation (50)
$\psi$	integral defined by equation (42)

SUBSCRIPTS

$e$	edge of boundary layer conditions
$f$	property of fuel
$i, j, m$	indices for $i$ th, $j$ th, or $m$ th the chemical species
$N$	property of atomic nitrogen
$O$	property of atomic oxygen
$O_2$	property of molecular oxygen
$P_1$	property of first product
$P_2$	property of second product
$w$	wall or body surface conditions

SUPERSSCRIPTS

$'$	reactant or fluctuating component
$''$	product
$*$	stoichiometric conditions

## SECTION 1

### INTRODUCTION

The study of combustion processes requires a blending of complex chemical and fluid dynamical phenomena. Under certain conditions the interactions between these fields can be minimized. For example, if the speed of chemical reactions is rate controlling, attention can be focused on chemical phenomena with little emphasis on the accompanying flow conditions. Here the most difficult problem to be faced is that of adequately describing the chemical kinetics. Generally, the detailed reaction steps are not well known, and even if they are it is unusual if the corresponding specific reaction rate coefficients are known within several orders of magnitude. This difficulty is often circumvented by assuming either very fast or very slow reactions. On the other hand, if diffusion and convection are rate controlling, prediction of combustion phenomena depends largely upon the state of knowledge for the particular viscous flow phenomenon involved.

Viscous flows can be classified as laminar, turbulent or transition; forced convection or free convection; boundary layer or wake flows. Of all the various combinations, laminar, forced convection, boundary layer flow lends itself most easily to mathematical description. Although turbulent flow is not nearly as well understood in detail, turbulent skin friction, mass transfer, and heat transfer, under conditions of forced convection boundary layer flow, can be predicted with some degree of success with the aid of a few empirical constants obtained from experiments. It certainly does not rank last among the various possible combinations of the above

phenomena. However, because the fundamentals remain rather obscure any attempt to make predictions is held in rather low esteem in some circles. Unfortunately, the engineer is faced with turbulent flow far more often than he can depend upon laminar flow. In the case under consideration, the combustion of chemically active sublimating surfaces, this is even more likely to be true. Both the high surface temperature and the surface mass injection should tend to destabilize the laminar boundary layer.

The laminar case was investigated by the author and Dr. D. A. Dooley, also of Aeronutronic Systems, Inc.<sup>(1)\*</sup> The present report should be regarded as a sequel to the previous work. Much the same approach is used in the present analysis. In the gas phase, diffusion is assumed to be rate controlling so that the chemical reactions chosen to represent the combustion process can be considered to be nearly in equilibrium. At the surface a somewhat more general treatment is used. The solid surface combustion and sublimation reactions are considered to proceed in such a way that the products are swept away by diffusion and convection faster than they are produced when the flux of species is high; while if the flux rate is low, the backscattering of products is sufficient to approximate equilibrium. This amounts to allowing either chemical reaction or diffusion to be rate controlling at the surface under appropriate circumstances.

In its boundary layer aspects the present semi-empirical theory uses an approach similar to that of Van Driest<sup>(2)(3)</sup> who allowed for variations in density through the boundary layer in such a manner that the results reduce to the von Kármán-Schoenherr relationship for incompressible skin friction. It has been pointed out that there are several formulations for including variable density which can be made to reduce to the incompressible results<sup>(9)(10)</sup> but Van Driest's physical reasoning seems to have been sufficiently good so that his results agree well with experiments.<sup>(3)</sup> It is hoped that an extension of this method to the case of combustion will meet with some measure of success. However, until experimental evidence is available the results obtained should be used with caution.

---

\* Since publication of that report a great deal of interest has been stimulated in this field. Papers by Lees<sup>(4)</sup> and by Cohen, Bromberg and Lipkis<sup>(5)</sup> treat similar chemical systems with similar results.



## SECTION 2

### TURBULENT BOUNDARY LAYER EQUATIONS

Although prediction of turbulent boundary layer phenomena, within the present state of knowledge, must be semi-empirical in nature, analysis of the fundamental equations helps form a logical framework for physical reasoning. The development of the fundamental equations rests on the conventional assumption that the conservation equations for a continuum hold instantaneously. The instantaneous value of each of the unknowns is separated into the sum of a mean and a fluctuating part. Introduction of such expressions into the conservation equations for reacting gas mixtures and averaging according to the Reynolds rules for time averages yield average conservation equations which include correlations between fluctuating components. The full equations which result are presented in Appendix A where the simplifications which can be made prior to introducing the boundary layer assumptions are discussed. As in the laminar analysis, it is assumed that diffusion due to temperature and pressure gradients is negligible compared to that due to concentration gradients and that all diffusion coefficients are equal. When correlations involving fluctuations in molecular transport terms are neglected according to the reasoning of Appendix A and boundary layer assumptions are made, i.e.,  $\partial/\partial y \gg \partial/\partial x$  and  $Re \gg 1$  small, the following boundary layer equations result in the mean steady state for blunt body coordinate systems:

Continuity for Molecular Species

$$\bar{\rho} u \frac{\partial \bar{\kappa}_i}{\partial x} + \bar{\rho} v \frac{\partial \bar{\kappa}_i}{\partial y} = \frac{\partial}{\partial y} \left( \bar{\rho} \bar{D} \frac{\partial \bar{\kappa}_i}{\partial y} - \overline{(\rho v)' \kappa_i'} \right) + \bar{w}_i \quad (1)$$

In this and the following equations the bars denote averages and the primes denote fluctuating components. The quantity  $\kappa_i$  is the mass fraction of the  $i$ th molecular species while  $w_i$  is its rate of production per unit volume.

Overall Continuity

$$\frac{\partial (\bar{\rho} u R_o^k)}{\partial x} + \frac{\partial (\bar{\rho} v R_o^k)}{\partial y} = 0 \quad (2)$$

where  $R_o$  is unity for bodies of revolution and zero for two dimensional bodies.

Continuity for Atomic Species

$$\bar{\rho} u \frac{\partial \bar{T}_m}{\partial x} + \bar{\rho} v \frac{\partial \bar{T}_m}{\partial y} = \frac{\partial}{\partial y} \left( \bar{\rho} \bar{D} \frac{\partial \bar{T}_m}{\partial y} - \overline{(\rho v)' T_m'} \right) \quad (3)$$

The atomic mass fractions,  $T_m$ , are related to the molecular mass fractions through the definition:

$$T_m = \sum_i \rho_{mi} \kappa_i \quad (4)$$

where  $\bar{n}_m$  represents the mass of atomic species  $m$  per unit mass of molecular species  $i$

#### Momentum

$$\bar{\rho} \bar{u} \frac{\partial \bar{u}/u_e}{\partial x} + \bar{\rho} \bar{v} \frac{\partial \bar{u}/u_e}{\partial y} = -\frac{\partial \bar{p}}{\partial x} \frac{1}{u_e} \left(1 - \frac{\bar{\rho} \bar{u} \bar{u}}{\bar{\rho}_e u_e^2}\right) + \frac{\partial}{\partial y} \left( \bar{\mu} \frac{\partial \bar{u}/u_e}{\partial y} - (\bar{\rho} v)' \frac{\bar{u}}{u_e} \right) \quad (5)$$

$$-\bar{\rho} \bar{u} \bar{u} \kappa = -\frac{\partial}{\partial y} (\bar{p} + (\bar{\rho} v)' v') \quad (6)$$

where  $\bar{\rho}_e$  and  $u_e$  are the density and velocity at the edge of the boundary layer. The second momentum equation indicates that the change in pressure across the boundary layer is small.

#### Energy

$$\begin{aligned} \bar{\rho} \bar{u} \frac{\partial \bar{h}_s}{\partial x} + \bar{\rho} \bar{v} \frac{\partial \bar{h}_s}{\partial y} = \frac{\partial}{\partial y} \left[ -(\bar{\rho} v)' \sum_i \bar{\kappa}_i \bar{h}_i' + \bar{\kappa} \frac{\partial \bar{T}}{\partial y} \right. \\ \left. + \sum_i \bar{h}_i \left\{ -(\bar{\rho} v)' \bar{\kappa}_i' + \bar{\rho} \bar{D} \frac{\partial \bar{\kappa}_i}{\partial y} \right\} \right. \\ \left. + \bar{u} \left\{ -(\bar{\rho} v)' \bar{u}' + \bar{\mu} \frac{\partial \bar{u}}{\partial y} \right\} \right] \quad (7) \end{aligned}$$

where the average total enthalpy is defined as  $\bar{h}_s = \sum_i \bar{\kappa}_i \bar{h}_i + \frac{\bar{u}^2}{2}$

and the enthalpy of each species,  $\bar{h}_i$ , includes the chemical enthalpy  $\bar{h}_i^0$ .

It is now useful to introduce eddy transport coefficients for turbulent flow.

$$-\overline{(\rho v)' u'} = \epsilon \frac{\partial \bar{u}}{\partial y} \quad (8)$$

$$-\overline{(\rho v)' \sum_i \bar{h}_i h_i'} = \kappa_T \frac{\partial \bar{T}}{\partial y} \quad (9)$$

$$-\overline{(\rho v)' \kappa_i'} = \bar{\rho} D_T \frac{\partial \bar{\kappa}_i}{\partial y} \quad (10)$$

It is to be noted that fluctuations in  $h_i'$  are due to temperature only so that the definition of equation (9) is reasonable. Prandtl and Lewis numbers for turbulent flow are then defined as:

$$Pr_T = \frac{\bar{c}_p (\bar{\mu} + \epsilon)}{\bar{\kappa} + \kappa_T} \quad (11)$$

$$Le_T = \frac{\bar{\rho} \bar{c}_p (\bar{D} + D_T)}{\bar{\kappa} + \kappa_T} \quad (12)$$

Because both the molecular and macroscopic transport properties arise from similar mechanisms for many gases it seems reasonable to assume that:

$$Pr_T = Le_T = 1 \quad (13)$$

Under these conditions it can be assumed that enthalpy and the atomic mass fractions are linear functions of the velocity ratio. With these assumptions, both the continuity equation for atomic mass fractions and the energy equation reduce to:

$$\bar{\rho} u \frac{\partial \bar{u}/u_e}{\partial x} + \bar{\rho} v \frac{\partial \bar{u}/u_e}{\partial y} = \sum_j \left[ (\bar{u} + \epsilon) \frac{\partial \bar{u}/u_e}{\partial y} \right] \quad (14)$$

This equation is identical with the momentum equation except for the term:

$$- \frac{\partial \bar{P}}{\partial x} \frac{1}{u_e} \left( 1 - \frac{\bar{\rho} u \bar{u}}{\bar{\rho}_e u_e^2} \right)$$

Although neglect of this term in the momentum equation will, probably have little effect on the velocity distribution in turbulent flow, the assumption of similarity between total enthalpy, atomic mass fractions and velocity ratio is somewhat questionable in regions of high pressure gradient. By the reasoning of Lees,<sup>(6)</sup> the term is probably negligible if the body surface is strongly cooled because the increase in density near the wall compensates for the decrease in velocity; therefore, the coefficient of the pressure gradient is small throughout the boundary layer. This argument should be viewed with some caution, however, because other combinations of terms could be devised such that the coefficient of the pressure gradient would be small throughout the boundary layer. Under these conditions

the terms retained in the momentum equation would not lead to similarity between the enthalpy, mass fractions and velocity ratio. The advantage of similarity is that once the velocity distribution is obtained, the use of the von Karman momentum integral equation alone is sufficient to estimate the skin friction, heat transfer and mass transfer at the surface. Otherwise the corresponding integral equations for energy and species continuity must also be solved.

SECTION 3  
CHEMICAL REACTIONS, MASS TRANSFER,  
AND HEAT TRANSFER

3.1 INTERACTION OF DIFFUSION AND CHEMICAL REACTIONS

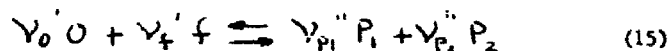
In a chemical system in which diffusion plays an important role, use of the continuity equations for atomic species is convenient for estimating mass transfer rates. However, because these equations are formed from linear sums of the molecular species equations they usually are not sufficient to completely replace the molecular species continuity equations. In other words, there are usually less atomic than molecular species. A discussion of the number of additional relationships required is given in Appendix B. These additional relationships are obtained by making some assumptions about the rates of production,  $\omega_i$ . As pointed out in reference 1, the specific reaction rate coefficients are usually not known to better than an order of magnitude. Therefore, the study of limiting cases through utilization of simplified models of the actual chemical kinetics is more profitable.

In the first place, it is assumed that some possible reactions do not occur at all. This entirely eliminates some of the possible molecular species from further consideration. In addition, two opposite limiting assumptions can be made about the rates of production,  $\omega_i$ . It might be assumed that the specific reaction rate coefficients are very small so that reactions can occur only at the solid boundary or outside the boundary layer. Under these conditions the molecular mass fractions can be obtained as linear functions

of the velocity ratio because the troublesome  $W_1$  terms can be neglected in equation (1). In most situations involving combustion, however, the high temperatures in the boundary layer probably lead to high rate coefficients. The opposite limiting case is to assume that these rate coefficients are very large compared to the production rates. Under these conditions the perturbation from equilibrium caused by diffusion and convection of species is small. Therefore, the mixture of gases at any point in the boundary layer can be determined from a knowledge of the atomic mass fractions,  $\bar{P}_m$ , and through use of expressions for the equilibrium constants of the various reactions. This procedure will be adopted for the remainder of this report. If the disturbance due to diffusion is of some importance it still may be convenient to use this approach for the first iteration in the computation procedure.

### 3.2 CHEMICAL MODEL

Although a more general treatment is possible, it is now assumed for simplicity that the surface material is a sublimator, i.e., it passes into the gaseous state without going through a liquid phase. In addition, it is assumed that it reacts with oxygen to form two possible products of combustion,  $P_1$  and  $P_2$ , but it does not combine with nitrogen. The possibility that oxygen and nitrogen may dissociate or recombine is also included, but formation of other species such as  $NO$  and ionized molecules is neglected. It was shown in reference 1 that these latter assumptions are adequate for air over a wide range of temperature. A set of possible reactions in the gas phase are then:





where  $f$  represents the surface material (fuel). It is further assumed that the fuel does not contain nitrogen, but may contain oxygen in addition to two atomic species,  $f_1$  and  $f_2$ . The equilibrium constants corresponding to the above reactions are given by:

$$K_{P_{f_1,2}} = \prod_j (P_j)^{\frac{y_j' - y_j''}{v_0}} \quad j = P_1, P_2, O, f \quad (18)$$

$$K_{P_O} = \frac{P_O^2}{P_{O_2}} \quad (19)$$

$$K_{P_N} = \frac{P_N^2}{P_{N_2}} \quad (20)$$

The partial pressures  $P_i$  are related to the mass fractions  $K_i$  through:

$$P_i = \frac{K_i}{M_i} M P \quad (21)$$

where  $M$  is the molecular weight of the mixture and  $P$  is the pressure for the mixture. The equilibrium constants  $K_{P_i}$  are usually known rather accurately as functions of temperature.

### 3.3 MASS TRANSFER AT SURFACE

The boundary condition at the surface for mass transfer can be stated in terms of conservation of atomic species:

$$\dot{n}_{mf} \dot{m}_w = \sum_i \dot{n}_{mi} \dot{m}_{iw} \quad (22)$$

where  $\dot{m}_w$  is the net flux of surface material, while  $\dot{m}_{i,w}$  is the net flux of molecular species  $i$  at the surface. For each reaction, conservation of atomic species leads to:

$$\sum_i (v_i'' - v_i') \alpha_{mi} = 0 \quad (23)$$

where  $\alpha_{mi}$  is the number of atoms of atomic species  $m$  per molecule of molecular species  $i$ . It is related to  $\rho_{mi}$  through  $\rho_{mi} = \alpha_{mi} M_m / M_i$ . Simultaneous solution of the sets of equations given by equations (22) and (23) has among the results the following expression of surface mass flow for the particular chemical system under consideration:

$$\dot{m}_w = \dot{m}_{f,w} - \frac{v_f' M_f}{v_o' M_o} (\dot{m}_{o,w} + \dot{m}_{o_2,w}) \quad (24)$$

This equation states that the net flux of surface material is equal to the sum of net fluxes due to the material which sublimates and that which enters into chemical reaction with oxygen at the surface.

The net flux rates consist of the difference between the flux of the species issuing from the surface and that which reacts with the surface. In other words:

$$\dot{m}_{i,w} = \dot{m}_{i,f} - \sigma_i \dot{m}_{i,b} \quad (25)$$

where  $\dot{m}_{i,f}$  is the flux of species  $i$  from the surface,  $\dot{m}_{i,b}$  is the flux striking the surface, and  $\sigma_i$  is the fraction of this back flux which reacts. In the case of the fuel  $\sigma_f$  is commonly known as the sticking factor or the accommodation coefficient. The back flux can be calculated easily from elementary kinetic theory<sup>(7)</sup>:

$$\dot{m}_{i,b} = \frac{P_{i,w}}{\sqrt{\frac{2\pi R_0 T_w}{M_i}}} \quad (26)$$

The outward rates can also be estimated, but they are better treated separately. In the case of the fuel, the outward rate is due to the sublimation process. The mass flow rate should depend principally upon the solid surface temperature and reduce to no net mass flow at equilibrium. Therefore:

$$\dot{m}_{f,+} = \frac{\nabla_f K_{Pf}}{\sqrt{\frac{2\pi R_0 T_w}{M_f}}} \quad (27)$$

Here, the quantity  $K_{Pf}$  is the equilibrium constant for sublimation. An expression of similar form could be deduced from the physics of the solid surface. The outward rate for oxygen has a somewhat more complex cause. In this case, some of the products produced by reaction between oxygen and the surface may encounter conditions in a microscopic layer near the surface such that they dissociate again and precipitate fuel species on the surface. The result is that oxygen is released into the boundary layer. Clearly, such a process must depend not only on the wall temperature, but also on the presence of the products. In order to reduce to no net flow at equilibrium, the expression for atomic oxygen is:

$$\dot{m}_{O_f} = \frac{\nabla_0 \prod (P_{j,w})^{v_j''/v_0'} K_{P_{P_{1,2}}}}{(K_{Pf})^{v_f''/v_0'} \sqrt{\frac{2\pi R_0 T_w}{M_O}}} \quad j = P_1, P_2 \quad (28)$$

Similar reasoning for molecular oxygen leads to:

$$\dot{m}_{O_{2f}} = \left[ \frac{K_{P_{P_{1,2}}} \prod (P_{j,w})^{v_j''/v_0'}}{(K_{Pf})^{v_f''/v_0'} K_{P_{O_2}}^{1/2}} \right]^2 \frac{\nabla_{O_2}}{\sqrt{\frac{2\pi R_0 T_w}{M_{O_2}}}} \quad (29)$$

Substitution of equations (25) through (29) in equation (24) leads to an expression for the net mass flow from the surface in terms of wall temperature and the partial pressures or mass fractions of the various species. Since equilibrium is assumed for the gas phase reactions, the mass fractions are related through equations (18), (19), and (20). Additional relationships are obtained from solutions of the boundary layer equations.

#### 3.4 ATOMIC MASS FRACTIONS AT SURFACE

If the Lewis number is unity and the atomic mass fractions are linear functions of the velocity ratio, then equation (22) leads to the following set of expressions for atomic mass fractions at the surface:

$$T_{mw} = \frac{T_{me} + \lambda_{mf} B}{1+B} \quad (30)$$

where

$$B = \frac{\dot{m}_w}{\rho_e u_e c_{pe}/2} \quad (31)$$

The quantity  $B$ , which represents the ratio of mass injection to skin friction or heat transfer coefficients, often appears in combustion literature. A further relationship between skin friction and  $B$  is obtained from a solution of the momentum equation which will be discussed in a later section for turbulent flow. The system of equations represented by equation (30) can be put in a more convenient form for the particular chemical system under consideration. Simultaneous solution of equations (30) and (23) leads to the following equations:

$$K_{Aw} + K_{N_2w} = \frac{T_{we}}{1+B} \quad (32)$$

$$\kappa_{i,w} = \frac{Y_i'' M_i}{Y_0' M_0} \left[ \frac{T_{0e}}{1+B} - (\kappa_{O,w} + \kappa_{O_2,w}) \right] \quad (33)$$

$i = P_1, P_2$

$$\kappa_{f,w} = \frac{B-B^*}{1+B} + \frac{Y_f' M_f}{Y_0' M_0} (\kappa_{O,w} + \kappa_{O_2,w}) \quad (34)$$

where

$$B^* = \frac{Y_f' M_f}{Y_0' M_0} T_{0e}$$

The above equations represent four relations among the eight unknowns:  $\kappa_{H,w}$ ,  $\kappa_{N,w}$ ,  $\kappa_{P,w}$ ,  $\kappa_{P_2,w}$ ,  $\kappa_{f,w}$ ,  $\kappa_{O,w}$ ,  $\kappa_{O_2,w}$ , and  $B$ . Three additional relations are supplied by the equilibrium relations of equations (18), (19), and (20). If  $\rho_e u_e c_{fe}/2$  is known, one additional relation is supplied by equations (24) through (29). Therefore all eight unknowns can probably be found as functions of pressure, wall temperature, and the quantity  $\rho_e u_e c_{fe}/2$ . Such relations apply to either laminar or turbulent flow. As mentioned previously, the connection between  $c_{fe}$  and the other variables for turbulent flow will be discussed in a later section.

### 3.5 HEAT TRANSFER

The heat absorbed by or radiated away from the surface,  $q_a$ , is obtained from a heat balance:

$$q_a = \left( \kappa \frac{\Delta T}{\Delta y} \right)_w - \sum_i \dot{m}_{i,w} h_{i,w} + \dot{m}_w h_{f,s} \quad (35)$$

The heat flux is due to conduction out of the boundary layer less the difference between heat convected by all individual species and that convected from the solid whose surface enthalpy is  $h_{f,s}$ . If  $Le = Pr = 1$  and the total enthalpy,  $h_s$ , is a linear function of the velocity ratio, then it can be shown that:

$$q_a = p_e u_e c_{pe}/2 [h_{se} - h_{sw} - B(h_{sw} - h_{fs})] \quad (36)$$

By making use of expressions (32), (33), and (34),  $q_a$  can be put in the following more illustrative form:

$$q_a = p_e u_e c_{pe}/2 [h_{se} + \alpha_w T_{0e} Q_{p0w} - h_{ew} - B\lambda_{fw}] \quad (37)$$

where

$$Q_{p0w} = \sum_i \frac{(V_i' - V_i'') M_i}{V_0' M_0} h_{i,w} + \epsilon_{ow} h_{ow} + (1 - \epsilon_{ow}) h_{o_2,w}$$

$i = F, P, P_2$

$$h_{ew} = T_{0e} (\epsilon_{nw} h_{nw} + (1 - \epsilon_{nw}) h_{n_2,w})$$

$$+ T_{0e} (\epsilon_{ow} h_{ow} + (1 - \epsilon_{ow}) h_{o_2,w})$$

$$\lambda_{fw} = h_{fw} - h_{fs}$$

$$\alpha_w = [1 - (1+B)(\kappa_{ow} + \kappa_{o_2,w})/T_{0e}]$$

$$\epsilon_{ow} = \kappa_{ow}/(\kappa_{ow} + \kappa_{o_2,w}) \quad \epsilon_{nw} = \kappa_{nw}/(\kappa_{nw} + \kappa_{n_2,w})$$

The quantity  $Q_{p0w}$  is the heat of combustion at wall conditions,  $h_{ew}$  is the enthalpy of air at wall conditions of temperature and dissociation, and  $\lambda_{fw}$  is the heat of sublimation. When there is no combustion or sublimation, both  $B$  and  $\alpha_w$  are zero, so that equations (36) and (37) reduce to the ordinary results for compressible flow with Prandtl number unity. If combustion takes place  $\alpha_w$  approaches unity because most of the oxygen is used up.

## SECTION 4

### ESTIMATION OF TURBULENT SKIN FRICTION

#### 4.1 VELOCITY DISTRIBUTION

Inspection of the momentum equation given by equation (5) shows that in the sublayer the shear must increase from the surface value due to the effect of mass injection at the surface. The increase in shear near the wall can be estimated by (8):

$$\tau = \tau_w (1 + \beta z)^\alpha \quad (38)$$

where

$$\tau = \bar{\mu} \frac{\partial \bar{u}}{\partial y} - \overline{(\rho v)' u'}$$

$$\beta = \frac{\dot{m}_w u_e}{\tau_w} = \frac{2 \dot{m}_w}{\rho_e u_e c_{fe}}$$

$$\dot{m}_w = (\rho v)_w$$

$$z = \bar{u}/u_e$$

The quantity  $\mathcal{E}$ , which has appeared in previous relationships, is a measure of the ratio of mass injection to skin friction or heat transfer. The exponent  $\alpha$  is introduced in order to trace the influence of the shear distribution on skin friction. Its value is unity. This shear distribution should be viewed with the same qualifications as apply to the constant shear assumption usually made for turbulent boundary layers with no blowing. The shear should approach zero at the outer edge of the boundary layer, but the influence of the velocity distribution in this region on the skin friction may be small.

In the fully turbulent region near the wall, it is assumed that, following Van Driest<sup>(2)</sup>:

$$\tau = -\bar{\rho} \overline{v'u'} \quad (39)$$

Introduction of the Prandtl mixing length,  $\ell$ , leads to:

$$\tau = \bar{\rho} \ell^2 \left| \frac{\partial \bar{u}}{\partial y} \right| \frac{\partial \bar{u}}{\partial y} \quad (40)$$

Either the assumption of Prandtl,  $\ell = \kappa y$ , or the von Kármán similarity law,  $\ell = \kappa (\partial \bar{u} / \partial y) / (\partial^2 \bar{u} / \partial y^2)$ , may now be introduced. It is assumed that these formulations, originally developed for incompressible flow with little  $\chi$  variation of fluid properties, apply to the present case. By integration of equation (40) with the Prandtl assumption, the velocity distribution is found to be given implicitly by:

$$y = \frac{v_w a}{\kappa u_e} e^{(a\psi - \kappa \bar{u})} \quad (41)$$



With the similarity law, the result is:

$$\eta_f = \frac{\gamma_w a}{\kappa u_\tau} e^{-\kappa F} \left[ a \int_0^z e^{a\psi} dz + 1 \right] \quad (42)$$

where

$$a = \kappa u_\tau \sqrt{\rho_w / \gamma_w}$$

$$\psi = \int_0^z \left[ \frac{\bar{p}}{\rho_w (1 + \beta z)^a} \right]^{1/2} dz$$

$$F = \text{Const.}$$

In both cases the arbitrary functions of  $X$  which result from integration have been chosen so that the velocity distribution reduces to that of incompressible flow with no blowing when the gas properties and shear do not vary. It has been pointed out by several writers<sup>(9)(10)</sup> that there are many formulations which could be made to reduce to the incompressible relations depending upon where properties in the functions of integration are evaluated. The above formulation follows that of Van Driest<sup>(2)</sup> who based these properties on wall conditions because of the strong influence of the wall in the sublayer. Justification can only come from a comparison with experiments. Van Driest's results for compressible flow on flat plates have given rather good agreement with experiments.<sup>(3)</sup>

The change in variable from  $\eta_f$  to  $z$ , at constant  $x$ , for use in the momentum integral is given by:

$$dy = \frac{\rho_w \bar{u}^2}{\rho_w u_e} e^{(u\psi - \kappa F)} \left[ \frac{\bar{\rho}}{\rho_w (1 + \beta z)^n} \right]^{\beta/2} dz \quad (43)$$

where  $\beta$  is zero if the von Kármán similarity law is used, and unity if  $l = \kappa y$

#### 4.2 SOLUTION OF MOMENTUM INTEGRAL FOR SKIN FRICTION

The von Kármán momentum integral, modified to include the effect of mass injection, can be obtained either by integration of the momentum equation across the boundary layer, neglecting double and triple correlations, or by consideration of momentum conservation for an element of fluid. The result is:

$$u_e \frac{d}{dx} \int_0^{\delta} \bar{\rho} \bar{u} \rho_o^R (1 - \bar{u}/u_e) dy = - \frac{d\rho}{dx} \int_0^{\delta} \left( \frac{\bar{\rho} \bar{u}^2}{\rho_e u_e^2} - 1 \right) \rho_o^R dy + \gamma_w \rho_o^R (1 + \beta) \quad (44)$$

where as before  $R$  is unity for bodies of revolution and zero for two-dimensional bodies. It is consistent with previous assumptions to neglect the first term on the right hand side of equation (44). In order to change the variable of integration to the velocity ratio,  $z$ , equation (43) is substituted in equation (44). The result can be put in the form:

$$\frac{D}{\kappa^3} a^2 \frac{d}{dx} (a^2 \rho_o^R J) = \frac{\rho_w u_e \rho_o^R (1 + \beta)}{\mu_w} \quad (45)$$

where

$$D = e^{-Kx}$$

$$J = \int_0^1 \bar{p}/p_w \left[ \frac{\bar{p}}{p_w(1+\beta z)^\alpha} \right]^{\beta/2} z(1-z) e^{a\psi} dz$$

The quantity  $a^2$  which appears in equation (45) is inversely proportional to the skin friction coefficient based on wall conditions. Since  $a^2$  is an unknown function of  $x$ , equation (45) cannot be integrated as it stands. However, at a sufficient distance from the stagnation point,  $a^2$  should be large. This permits certain approximations to be made. Change of variable from  $z$  to  $\psi$  makes it possible to express the integral  $J$  as:

$$J = \int_0^{\psi_e} f e^{a\psi} d\psi \quad (46)$$

where

$$f = (\bar{p}/p_w) z(1-z) \left[ \frac{\bar{p}}{p_w(1+\beta z)^\alpha} \right]^{\frac{\beta-1}{2}}$$

Successive integration of  $J$  by parts produces:

$$J = \left[ \frac{e^{a\psi}}{a} \sum_{n=0}^{\infty} \frac{(-1)^n}{a^n} \frac{d^{(n)} f}{d\psi} \right]_0^{\psi_e} \quad (47)$$

For large  $a$  with  $\psi_e$  of order unity the dominant term yields:

$$J \approx \frac{1}{a^2} e^{a\psi_e} (1+\beta)^\alpha \left[ \frac{p_w}{p_e} (1+\beta)^\alpha \right]^{-\beta/2} \quad (48)$$

In addition, it can be shown that if  $\alpha \psi_e$  is large:

$$(\alpha \psi_e)^2 \frac{d}{dx} g(x) e^{\alpha \psi_e} \approx \frac{d}{dx} [(\alpha \psi_e)^2 g(x) e^{\alpha \psi_e}] \quad (45)$$

Equation (45) can now be integrated approximately by making use of equations (48) and (49). The result gives a law for variation of turbulent skin friction:

$$\frac{\phi}{c_{fe}^{1/2}} = \frac{1}{2^{1/2} K} \left[ \ln \frac{\pi}{2D} + \ln \left\{ c_{fe} \tilde{Re}_{wT} \left( \frac{\rho_e}{\rho_w} \right)^{1-\frac{\beta}{2}} (1+\beta)^{1-\alpha(1-\frac{\beta}{2})} \right\} \right] \quad (50)$$

where 
$$\phi = \int_0^1 \left[ \frac{\bar{p}}{\rho_e (1+\beta z)^n} \right]^{1/2} dz$$

$$\tilde{Re}_{wT} = \frac{\int_0^\pi \psi_e^2 \rho_w u_e \rho_0^k dx}{\psi_e^2 \mu_w \rho_0^k}$$

It has been assumed that the influence of wall temperature and mass fraction variations in the  $x$  direction is negligible. If, in addition, it is assumed that the variation of  $\psi_e$  is not significant in determining the skin friction, the effective Reynolds number becomes:

$$\tilde{Re}_{WT} \approx \frac{\int_0^x \rho_w u_e \eta_0^{\beta} dx}{\mu_w \eta_0^{\beta}} \quad (51)$$

This Reynolds number reduces to the ordinary Reynolds number based on wall conditions for a flat plate. For a conical geometry, where  $\eta_0 = Cx$ , it becomes half the ordinary Reynolds number consistent with a derivation by Van Driest<sup>(11)</sup> for the conical geometry. The quantity  $\phi$  is unity for incompressible flow with no mass injection. For compressible flow with constant specific heat and no mass injection,  $\phi$  reduces to Van Driest's result when the enthalpy velocity variation is introduced. In the case of combustion, the evaluation of  $\phi$  is much more complicated due to the influence of variations in the gas mixture through the boundary layer which affect the relationships between density, enthalpy and velocity ratio. A method for obtaining  $\phi$  is discussed in Section 4.3 and calculations of  $\phi$  for the case of graphite combustion are described in Section 5.3.

Equation (50) shows clearly the influence of shear variation and mixing length assumptions on the skin friction through the exponents  $\alpha$  and  $\beta$ . As is well known, both mixing length formulations lead to the same result for incompressible flow with no mass injection. Equation (50) has the same form as the incompressible von Karman-Schoenherr law for skin friction. Two arbitrary constants,  $K$  and  $D$ , appear which must be obtained from experiments. If these constants are assumed to be the same as those obtained for the incompressible case, then equation (50) can be expressed as:

$$\frac{\phi}{C_{f0}^{1/2}} = 1.70 + 4.15 \log_{10} \left\{ C_{f0} \tilde{Re}_{WT} \left( \frac{\eta_0}{\rho_w} \right)^{1-\beta_2} (1+\beta) \right\}^{1-\alpha(1-\beta_2)} \quad (52)$$

It would be truly fortunate if these constants do not have to be adjusted.

It should be pointed out that because of the assumption of large  $\alpha$  the skin friction law does not apply at the stagnation point of blunt bodies. In this region, the above formulation leads to finite shear stress and infinite heat transfer, both of which are physically unsound. However, since the flow will probably not become turbulent until at least some small distance from the stagnation point, the behavior in this region is not as important as in the case of laminar flow.

### 4.3 EFFECT OF CHEMICAL STRUCTURE OF BOUNDARY LAYER ON INTEGRAL $\phi$

All of the results obtained so far, except for evaluation of the integral  $\phi$ , have required only evaluation of fluid properties at the body surface or at the edge of the boundary layer. In the case of laminar flow with assumptions similar to those made in the present investigation, no detailed knowledge of the chemical structure of the boundary layer is required in order to estimate heat transfer, mass transfer and skin friction. However, with turbulent flow, it is not possible to make the same transformations of the boundary layer equations, because the transport coefficients are not properties of the fluid but depend on the flow field. Fortunately, with the assumptions which have been made, the only difficult quantity to compute is the integral  $\phi$ . Its evaluation requires a knowledge of the density variation through the boundary layer.

When diffusion and chemical reactions occur in the boundary layer, the density varies not only because of temperature variations, but also because of changes in chemical composition. The temperature itself is related to the enthalpy, which is known in terms of the velocity ratio in a rather complicated implicit fashion. Not only is  $\phi$  more complicated to compute, but in addition, it depends upon more independent parameters.

$$\phi = \phi \left( h_{sw}/h_{se}, u_{\infty}^2/2h_{se}, T_w, P, B \right)$$

The last three parameters must be added in order to determine the composition throughout the boundary layer. Apparently, a simple graphical representation of  $\phi$  is not possible. However, the integrand of  $\phi$  can be determined if the enthalpy, pressure, and gas composition are known.

Fortunately, with the assumptions of fast reaction rates in the gas phase and  $Le = 1$ , the gas composition can be determined in terms of a single parameter,  $\xi$ . This can be seen through use of equation (30) for the atomic mass fractions at the surface and use of a linear relationship with the velocity ratio. Introduction of the parameter  $\xi$ , defined below, then yields the following expression for atomic mass fractions at any point:

$$T_m = \left( \alpha_m \xi \frac{M_m}{M_f} - T_{me} \right) \xi + T_{me} \quad (53)$$

where  $\xi = (1-z) \frac{B}{1+B}$

In order to actually compute the density variation, the molecular mass fractions must be found. These are obtained by simultaneous solution of equations (53) and (23). For the chemical system under consideration in this report the results are:

$$\kappa_f = \xi - B^* (1-\xi) + \frac{v_t' M_t}{v_0' M_0} (\kappa_0 + \kappa_{O_2}) \quad (54)$$

$$\kappa_i = \frac{v_i'' M_i}{v_0' M_0} [T_{0e} (1-\xi) - (\kappa_0 + \kappa_{O_2})] \quad (55)$$

$$\kappa_N + \kappa_{N_2} = T_{Ne} (1-\xi) \quad i = P_1, P_2 \quad (56)$$

In addition to these expressions, the equilibrium constants given by equations (18), (19), and (20) serve to determine the system.

The relationship between  $\xi$  and the velocity ratio in the boundary layer depends on the wall conditions of mass transfer which determine  $B$ . When the molecular composition is obtained at each location in the boundary layer, then the integrand of  $\phi$  can be evaluated in terms of enthalpy and pressure and  $\phi$  computed numerically from:

$$\phi = \left[ \frac{P}{\rho_e (1+B)^a} \right]^{1/2} \int_0^1 \left[ \frac{\bar{P}}{P(1-\xi)^a} \right]^{1/2} d\xi \quad (57)$$

It should be noted that the enthalpy is related to the wall and free stream boundary conditions and the velocity ratio,  $Z$ , through:

$$\bar{h} = (h_{se} - h_{sw}) Z + h_{sw} - \frac{u_e^2}{2} Z^2 \quad (58)$$

As stated above:

$$\left[ \frac{\bar{P}}{P(1-\xi)^a} \right]^{1/2} = f(P, \bar{h}, \xi) \quad (59)$$

The numerical computations are aided by determining the integrand  $f$  as a function of pressure and enthalpy at various fixed values of  $\xi$ . It can be seen from the definition of  $\xi$  that it is zero at the outer edge of the boundary layer and increases toward the surface when there is mass injection. The surface value of the composition parameter,  $\xi_w = B/(1+B)$ , can be obtained in terms of the mass transfer conditions at the surface. Under assumptions previously made, its value depends upon wall temperature, pressure, and the parameter  $\rho_e u_e C_{e/2}$ . Thus evaluation of  $\phi$  requires simultaneous solution of equations (52) and (57).



In addition to  $\xi_w$  another important value of  $\xi$  is that which occurs at the place where the reactants are in stoichiometric proportion. Equation (54) shows that this value of  $\xi$  is given by:

$$\xi^* = \frac{B^*}{1 + B^*} \quad (60)$$

This value of  $\xi$  occurs in the interior of the combustion zone, a region where the major portion of the combustion reaction takes place. For most combustion reactions the equilibrium constant given by equation (18) is very small for the environmental conditions which occur. Therefore, in the combustion zone the mass fractions of the reactants are small. Under these conditions the model of reference 1 is well approximated. The boundary layer is divided into two regions by a thin combustion zone. On one side of this zone oxygen is mixed with products and inerts while on the other side fuel is mixed with products and inerts. An estimate of the thickness of the combustion zone for the case where combustion takes place in the gas phase is given in Appendix C. If wall conditions are such that the reactants are in stoichiometric proportion at the surface, then  $\xi_w = \xi^*$ . At lower values of  $\xi_w$  the excess of oxygen increases at the wall until finally the combustion reaction does not take place at all if  $\xi_w = 0$ .

## SECTION 5

### COMBUSTION OF GRAPHITE

#### 5.1 CHEMICAL CONSIDERATIONS

As in reference 1 the combustion of graphite is investigated numerically because a great deal of data is available on this substance. The combustion process is assumed to be adequately described by the single reaction step:



The formation of  $CO_2$  which will only occur in appreciable quantities at low temperatures is neglected. In conformity with previous assumptions reaction with nitrogen which requires extremely high temperatures is also neglected. In addition, the form of the carbon molecule in the gaseous state is assumed to be monatomic, although recent experiments, (12)(13) indicate the possibility of  $C_3$  formation during sublimation. Since this question is not entirely settled, the simpler configuration is assumed for purposes of illustration. All of the above complications could be included with slight modification of the analysis.

The basic data listed in Table I of reference 1 are utilized for the present calculations. Additional data are required because of the somewhat more general treatment of the combustion

process in the present analysis. Equilibrium constants fitted empirically to data of reference (14) are as follows:

$$P_c = K_{P_c} \cong 1.3596 \times 10^8 e^{-\frac{1.55372 \times 10^5}{T}} \quad (62)$$

$$\frac{P_c P_o}{P_{CO}} = K_{P_{CO}} \cong 3.0172 \times 10^7 e^{-\frac{2.37607 \times 10^5}{T}} \quad (63)$$

The equilibrium constants are in atmospheres while the temperature is in degrees Rankine.

The sticking factor or accommodation coefficient,  $\gamma$ , for graphite sublimation is taken as 0.3. This fits the data of references (15) and (16) over a moderate temperature range (up to about 3000°K) assuming that the vapor is monatomic carbon. In reality the accommodation coefficient probably varies with temperature but the single constant value is consistent with the present state of knowledge. The value of  $\gamma$  for monatomic oxygen is assumed to be unity while that for diatomic oxygen is chosen at the two extremes, zero and unity, for purposes of illustration. Specially designed experiments are required in order to determine these coefficients.

## 5.2 GENERAL SURFACE MASS AND HEAT TRANSFER

Calculations have been made for graphite by means of several IBM 650 programs using the analytical results obtained in Section 3. Since nonequilibrium surface conditions have been considered, it is necessary to know a flow parameter in addition to surface temperature and pressure in order to specify the burning rate. This parameter,  $\rho_e u_e C_{te}/2$ , is a measure of the transport of properties to or from the wall. For a particular body geometry with given local free stream conditions as well as wall temperature and pressure this parameter can be obtained through use of the skin friction law of equation (52) for turbulent flow in conjunction with

equations (18) through (20), (24) through (29), and (32) through (34) for the mass fractions at the surface and B. In this section the quantity  $B$  is treated as an independent variable so that the results apply to any geometrical configuration in laminar or turbulent flow. All of the above named equations except equation (52) are utilized. In Section 5.5 calculations are described for the particular case of a hemisphere in turbulent flow.

In Figure 1 the mass injection parameter,  $B$ , is presented as a function of wall temperature, flow parameter, and accommodation coefficient for a fixed pressure of one atmosphere. The entire region below  $B = B^*$  represents conditions under which the combustion process is controlled by chemical reaction at the surface. In this region an appreciable quantity of oxygen is not consumed by the reaction. At low temperatures the value of the accommodation coefficient for molecular oxygen has considerable influence on the burning rate while at higher temperatures, when most of the oxygen becomes dissociated, it has little effect. All of the curves swing almost vertically upward at still higher temperatures due to the sublimation of gaseous carbon. The sublimation rate eventually becomes sufficiently large to drive the combustion zone away from the surface so that  $B > B^*$ . Under these conditions the diffusion of oxygen toward the wall is not sufficient to consume the flux of carbon coming off due to sublimation.

The lower values of the flow parameter result in higher values of  $B$ . When the flow parameter becomes sufficiently low it has no influence at all so that equilibrium is approximated. At high values of the flow parameter the quantity  $B$  becomes very small. This dependence of  $B$  on the flow parameter has a significant effect on the heat transfer rate given by equation (37). The factor  $\gamma$  exhibits a similar behavior as shown in Figure 2. The net effect of these factors is presented in Figure 3, where a portion of the enthalpy potential, namely,  $\Delta H$ , is presented as a function of the wall temperature and flow parameter at one atmosphere pressure. The flow parameter actually has the opposite effect on the surface mass loss as shown in Figure 4. Higher values of the flow parameter result in higher surface mass losses.

The effect of pressure on  $B$ ,  $\gamma$ , and enthalpy potential is shown in Figures 5, 6 and 7. Increased pressure has an effect similar to that of decreased flow parameter. Equilibrium is more nearly approached because of backscattering toward the surface.

5.3 EVALUATION OF THE INTEGRAL  $\phi$  FOR GRAPHITE IN AIR

By making use of equations (54) through (56) in addition to equations (18) through (20) the molecular mass fractions  $K_i$  can be obtained as functions of temperature and pressure for constant values of  $\xi$ . The enthalpy of the mixture can be substituted for temperature as a variable. Therefore, the integrand,  $[\bar{P}/P(1-\xi)^{\alpha}]^{1/2}$ , which occurs in the expression for  $\phi$  given by equation (57) can be found as a function of the enthalpy of the mixture and the pressure. Since the molecular species are forced to include C, CO, O, O<sub>2</sub>, N, and N<sub>2</sub> the enthalpy of the mixture will not necessarily be zero at zero temperature because of the heats of formation of C and CO. A shift of this datum so that all enthalpies are zero at zero temperature makes it possible to obtain a universal curve for the integrand of  $\phi$  over a considerable range of pressure, enthalpy and  $\xi$ . The heat of formation for the mixture can be approximated by expressions linear in  $\xi$ . When  $\xi \leq \xi^*$ ,  $K_L \approx 0$  at low temperatures so that from equations (54) and (55):

$$\xi \leq \xi^* \quad h^0 \approx \frac{M_{CO}}{M_L} h_{CO}^0 \xi \quad (64)$$

If  $\xi \geq \xi^*$ ,  $(K_O + K_{O_2}) \approx 0$  so that:

$$\xi \geq \xi^* \quad h^0 \approx \left[ (1+B^*) h_C^0 - \frac{M_{CO}}{M_O} T_{CO} h_{CO}^0 \right] \xi - \left[ h_C^0 B^* - \frac{M_{CO}}{M_O} T_{CO} h_{CO}^0 \right] \xi^* \quad (65)$$

The relevant numbers for graphite have been substituted for the heats of formation and the results of calculations for the integrand using the full set of equations (54) through (56) and (18) through (20) with the mixture heat of formation subtracted out have been plotted in Figure 8. Values of  $\xi$  equal to zero which represents air,  $\xi^*$  which represents the combustion zone, and  $2\xi^*$  which represents a fuel rich condition were chosen.

A fit to this distribution was obtained by adding a correction term to that which results for air treated as a perfect gas. The expression for the fit is as follows:

$$\left[ \frac{\bar{S}}{P(h)} \right]^{1/2} \approx \frac{0.0671}{H^{1/2}} + 0.48 \times 10^{-5} (H)^{1/2} \quad (66)$$

( $H = h - h^0$ )

where  $H$  is the enthalpy with a shifted datum given in BTU/lb. A slightly better fit may have been obtained with another form for the correction term, but the one chosen allows easy analytical integration of  $\phi$ .

The result of integration is as follows:

If  $B \leq B^*$

$$\phi = F \left[ \left( 1 + 0.715 \times 10^{-4} \frac{\{b_1^2 + 4a_1c_1\}}{8c_1} \right) \frac{1}{c_1^{1/2}} \left( \frac{\sin^{-1}(2c_1 - b_1)}{\sqrt{b_1^2 + 4a_1c_1}} + \sin^{-1} \frac{b_1}{\sqrt{b_1^2 + 4a_1c_1}} \right) \right. \\ \left. + 0.715 \times 10^{-4} \left\{ \frac{2c_1 - b_1}{4c_1} (h_0)^{1/2} + \frac{b_1}{4c_1} a_1^{1/2} \right\} \right] \quad (67)$$

If  $B \geq B^*$

$$\phi = F \left[ \left( 1 + 0.715 \times 10^{-4} \frac{\{b_2^2 + 4a_2c_2\}}{8c_2} \right) \frac{1}{c_2^{1/2}} \left( \frac{\sin^{-1}(2c_2 - b_2)}{\sqrt{b_2^2 + 4a_2c_2}} + \sin^{-1} \frac{b_2}{\sqrt{b_2^2 + 4a_2c_2}} \right) \right. \\ \left. + 0.715 \times 10^{-4} \left\{ \frac{(2c_2 - b_2)(H^*)^{1/2}}{4c_2} + \frac{b_2(c_2)^{1/2}}{4c_2} \right\} \right. \\ \left. + \left( 1 + 0.715 \times 10^{-4} \frac{\{b_1^2 + 4a_1c_1\}}{8c_1} \right) \frac{1}{c_1^{1/2}} \left( \frac{\sin^{-1}(2c_1 - b_1)}{\sqrt{b_1^2 + 4a_1c_1}} + \sin^{-1} \frac{(b_1 - 2c_1z^*)}{\sqrt{b_1^2 + 4a_1c_1}} \right) \right. \\ \left. + 0.715 \times 10^{-4} \left\{ \frac{(2c_1 - b_1)(h_c)^{1/2}}{4c_1} + \frac{(b_1 - 2c_1z^*)(H^*)^{1/2}}{4c_1} \right\} \right] \quad (68)$$

$$\text{where } F = \frac{h_e^{1/2}}{(1+B)^{1/2} (1 + 0.715 \times 10^{-4} h_e)}$$

$$a_1 = h_{sw} + 4020.1 \frac{B}{1+B} \quad a_2 = (h_{sw} - 30,441.3 \frac{B}{1+B}) + 5127.1$$

$$b_1 = h_{se} - a_1$$

$$b_2 = h_{se} - a_2 + 5127.1$$

$$c_1 = \frac{u_e^2}{2}$$

$$c_2 = \frac{u_e^2}{2}$$

$$H^* = a_1 + b_1 z^* - c_1 z^{*2}$$

$$z^* = \frac{B - B^*}{B(1+B^*)}$$

Although the above expressions for  $\phi$  appear rather formidable they actually represent a great simplification in that they are analytic. As pointed out in Section 4.3  $\phi$  is a function of five independent parameters.

It should be noted that when  $B = 0$  equation (67) gives a relationship for turbulent flow of air over nonreacting surfaces including the effects of dissociation. At low temperatures under these conditions the results reduce to those of Van Driest.<sup>(2)</sup>

## 5.4 INVISCID FLOW FIELD FOR BLUNT BODIES

For purposes of illustration heat and mass transfer on a hemisphere will be described in Section 5.5. The hemisphere is a simple geometry representative of blunt body shapes. A detailed investigation of the inviscid flow field on blunt bodies is beyond the scope of this report but it deserves attention because turbulent heat and mass transfer are more sensitive to the flow field than the laminar rates. A review and extension of this problem was recently presented by Van Dyke.<sup>(17)</sup> He points out that for the hemisphere, modified Newtonian flow as proposed by Lees<sup>(18)</sup> gives good agreement with his more elaborate numerical calculations, at least up to about fifty or sixty degrees. Lees<sup>(18)</sup> also presents some experimental correlation with Newtonian flow for the hemisphere. In view of these comments it appears that use of modified Newtonian flow on a hemisphere gives an adequate description of the pressure distribution for use in illustrating the heat and mass flux distribution. The pressure distribution is therefore given in terms of angular distance from the stagnation point by:

$$P/P_{T2} = P_1/P_{T2} + (1 - P_1/P_{T2}) \cos^2 \theta \quad (69)$$

The pressure ratio,  $P_{T2}/P_1$ , across the normal shock is affected very little by dissociation. However, there is a strong effect on the density ratio,  $\rho_{T2}/\rho_1$ , which is required in order to determine the heat transfer. Plots of the variation of these quantities with free stream velocity and altitude is given by Feldman in reference 19. The pressure and density serve to determine the state of the gas at the stagnation point. In order to determine conditions at some other point on the body the assumption that the air entering the boundary layer is at approximately the same entropy level can be used in addition to equation (69) for the pressure distribution. Other thermodynamic variables can then be determined from Mollier charts. However, when pressure variations are moderate an approximate method is simpler. This method consists of introducing a polytropic pressure density variation at constant entropy, i.e.,  $P/\rho^{\gamma_e} = \text{const.}$  where the exponent  $\gamma_e$  is defined by:

$$\gamma_e = \left( \frac{\partial \ln P}{\partial \ln \rho} \right)_s \quad (70)$$



A plot\* of  $\gamma_e$  vs free stream velocity is given in Figure 9 for the pressure limits shown. The value of  $\gamma_e$  is only of importance in regions far away from the stagnation point because at small distances the density is approximately constant.

With these assumptions the local mass flow and kinetic energy which occur in the heat transfer expression are given by:

$$\frac{\rho_e u_e}{\rho_1 u_1} = \left( \frac{P}{P_{T2}} \right)^{\frac{1}{\gamma_e}} \frac{P_{T2}}{P_1} \left[ \frac{\gamma_e}{\gamma_e - 1} \frac{P_1}{P_{T2}} \frac{P_{T2}}{P_1} \frac{2}{\gamma_1 M_1^2} \right]^{\frac{1}{2}} \left[ 1 - \left( \frac{P}{P_{T2}} \right)^{\frac{\gamma_e - 1}{\gamma_e}} \right]^{\frac{1}{2}} \quad (71)$$

$$\frac{u_e^2}{2 h_{se}} = \left( \frac{\gamma_e}{\gamma_e - 1} \right) \left( \frac{\gamma_1 - 1}{\gamma_1} \right) \frac{P_1}{P_{T2}} \frac{P_{T2}}{P_1} \frac{T_1}{T_{T2}} \left[ 1 - \left( \frac{P}{P_{T2}} \right)^{\frac{\gamma_e - 1}{\gamma_e}} \right] \quad (72)$$

Another required quantity is the effective Reynolds number for use in obtaining the skin friction coefficient. For the von Kármán similarity law, with  $\beta = 0$ , this parameter for a hemisphere is given by:

$$\tilde{R} = \frac{\left( \frac{\rho}{\rho_w} \right) \tilde{R}_{ewr} \frac{\mu_w}{\mu_1}}{\rho_{e,12} \left( \frac{P_{T2}}{P_1} \frac{P_{T2}}{P_1} \frac{2}{\gamma_1 M_1^2} \right)^{\frac{1}{2}}} = \frac{\left( \frac{\gamma_e}{\gamma_e - 1} \right)^{\frac{1}{2}} \int_0^\theta \frac{P}{P_{T2}} \left[ 1 - \left( \frac{P}{P_{T2}} \right)^{\frac{\gamma_e - 1}{\gamma_e}} \right]^{\frac{1}{2}} \sin \theta d\theta}{\left( \frac{P}{P_{T2}} \right)^{\frac{\gamma_e - 1}{\gamma_e}} \sin \theta} \quad (73)$$

\* The author is indebted to Dr. S. Lampert of Aeronutronic Systems, Inc. for supplying this graph.

In arriving at this relationship variations in wall temperature and molecular weight along the body have been neglected. The quantity  $Re_{\infty}$  is the free stream Reynolds number based on the radius of the hemisphere. The parameter  $\hat{R}$  is plotted as a function of Mach number and position in Figure 10. If the wall temperature and the free stream conditions upstream of the shock are known the effective Reynolds number,  $(\rho_e/\rho_w)\hat{R}_{ewT}$ , can be found at any body location.

### 5.5 HEAT AND MASS TRANSFER DISTRIBUTIONS ON A HEMISPHERE

Without adequate experimental data it is too much to expect that the present semi-empirical analysis will give accurate quantitative predictions of heat and mass transfer. However, if good judgment has been used in choosing the important chemical reactions and making physical assumptions, the trend of these phenomena may be predicted by making use of the analysis.

Forced convection heat transfer on blunt bodies with nonreacting surfaces exposed to hypersonic inviscid flow conditions has received considerable attention in recent years. It is therefore interesting to determine what the heat and mass transfer distributions may be under similar external flow conditions when the surface reacts with the environment. The combustion of a graphite hemisphere exposed to free stream conditions corresponding to Mach 10 flight at altitudes of 100,000 or 50,000 ft has been chosen as an example. In addition to Mach number and altitude, the free stream Reynolds number and the wall temperature must be given in order to specify the heat and mass transfer. Two Reynolds numbers an order of magnitude different have been chosen for each altitude. The wall temperature was varied from 2000 to 8000°R. Some assumptions about the accommodation coefficients must also be made. These were chosen as  $\gamma_c = 0.3$ ,  $\gamma_o = 1$ , and  $\gamma_{O_2} = 0$  for purposes of illustration.

In order to carry out the computations the inviscid flow field considerations of Section 5.4 were combined with equations (18) through (20), (24) through (29), and (32) through (34) for the mass fractions at the surface  $B$ ; equation (52) for the turbulent skin friction law; equations (67) and (68) for  $\phi$ ; and equation (37) for the heat transfer. Use of the turbulent skin friction law eliminates the flow parameter,  $\rho_e u_e c_{fe} / \lambda$ , as an independent parameter for the particular case being studied. The computations were accomplished by means of an IBM 650 program.

Figures 11 through 14 contain distributions of heat flux, mass flux,  $B$  and  $\alpha_w$ , respectively, for the 100,000 ft altitude while Figures 15 through 18 contain corresponding distributions for the 50,000 ft altitude. Comparison of these curves shows that the level of both heat transfer and mass flux is almost an order of magnitude higher at the lower altitude at approximately the same Reynolds number and surface temperature. This is due to the strong influence of the free stream density in turbulent flow which is reflected in the local value of  $\rho_e u_e$ . Because the skin friction is only slightly affected by variations in Reynolds number, the heat and mass transfer rates vary little with Reynolds number at low temperature. At high temperature the general heat and mass transfer plots of Figures 3 and 4 indicate that there is much more sensitivity to the flow parameter for  $\gamma_{O_2} = 0$ . Therefore, variations in Reynolds number have a moderate influence at high temperature as shown in Figures 11 through 18.

The heat flux variations between 6000 and 8000°R shown in Figure 11 for the 100,000 ft altitude show a rather confusing pattern which can be explained, however, by a comparison with the corresponding conditions for  $B$  and  $\alpha_w$  presented in Figures 13 and 14. The confusion in this temperature range is caused by the rapid occurrence of gas phase combustion as illustrated by Figure 13 and the rapid consumption of oxygen at the surface as shown by Figure 14 when the temperature is increased. The heat flux variations at 50,000 ft display a more regular appearance as shown in Figure 15 because gas phase combustion is not approached in the temperature range shown. The prevention of gas phase combustion at the lower altitude is primarily due to the effect of increased flow parameter.

At low temperatures the heat flux distributions in both Figures 11 and 15 exhibit a peak value in the vicinity of 40 degrees on the hemisphere. This behavior is characteristic of turbulent heat flux distributions on non-reacting blunt bodies at hypersonic speeds. Under these conditions the enthalpy potential is only slightly affected by surface conditions and the skin friction coefficient varies moderately with geometrical location. Thus, the flow parameter,  $\rho_e u_e C_{f,2}/2$ , and hence the heat transfer reflect the variation in  $\rho_e u_e$  around the body.

The mass flux variations shown in Figures 13 and 16 also exhibit a peak flux near 40 degrees in many cases in spite of a different shape in the  $B$  distributions of Figures 14 and 17.

In Figure 19 the variation of the integral  $\phi$  around the body is shown. The value of  $\phi$  is remarkably close to unity, the incompressible value. This is because at high temperatures the integrand of  $\phi$  is mainly in the flat portion of the curve shown in Figure 8 throughout the boundary layer.

# LIST OF REFERENCES

1. Denison, M. R. and Dooley, D. A.; Combustion in the Laminar Boundary Layer of Chemically Active Sublimators, Aeronutronic Systems, Inc., Technical Report U-110, 23 September 1957.
2. Van Driest, E. R.; "Turbulent Boundary Layer in Compressible Fluids," Journal of the Aeronautical Sciences, Vol. 18, No. 3, March 1951.
3. Van Driest, E. R.; "The Problem of Aerodynamic Heating," Aeronautical Engineering Review, October 1956.
4. Lees, L.; Convective Heat Transfer with Mass Addition and Chemical Reactions, Paper presented at Third Combustion and Propulsion Colloquium AGARD, NATO, Palermo, Sicily, 17-21 March 1958.
5. Cohen, C. B., Bromberg, R., and Lipkis, R. P.; Boundary Layers with Chemical Reactions Due to Mass Additions, The Ramo-Wooldridge Corporation, Report GM-TR-268, 1 October 1957.
6. Lees, L.; "Laminar Heat Transfer over Blunt-Nosed Bodies at Hypersonic Flight Speeds," Jet Propulsion, Vol. 26, No. 4, April 1956.
7. Mayer, J. E. and Mayer, C. M.; Statistical Mechanics, pp. 17-18, John Wiley & Sons, Inc., New York, 1940.
8. Dorrance, W. H., and Dore, E. J.; "The Effect of Mass Transfer on the Compressible Turbulent Boundary Layer Skin Friction and Heat Transfer," Journal of the Aeronautical Sciences, Vol. 21, No. 6, June 1954.
9. Howarth, L.; Modern Developments in Fluid Dynamics - High Speed Flow, pp. 456, Oxford at the Clarendon Press, 1953.
10. Chapman, D. R. and Keeter, R. H.; "Measurements of Turbulent Skin Friction on Cylinders in Axial Flow at Subsonic and Supersonic Velocities," Journal of the Aeronautical Sciences, Vol. 20, No. 7, July 1953.
11. Van Driest, E. R.; "Turbulent Boundary Layer on a Cone in a Supersonic Flow at Zero Angle of Attack," Journal of the Aeronautical Sciences, Vol. 19, No. 1, January 1952.

12. Brewer, L., Gillies, P. W., and Jenkins, F. A.; "The Vapor Pressure and Heat of Sublimation of Graphite," Journal of Chemical Physics, 16, 797 (1948).
13. Chupka, W. A., and Inghram, M. C.; "Molecular Species Evaporating from a Carbon Surface," Journal of Physical Chemistry, 21, 1313, (1953).
14. Gordon, J. S.; Thermodynamics of High-Temperature Gas Mixtures, and Application to Combustion Problems, WADC Technical Report 57-33, January 1957.
15. Farber, M., and Darnell, A. J.; "The Vaporization of Graphite Filaments," Journal of American Chemical Society, 74, 3941 (1952).
16. Marshall, A. L. and Norton, F. J.; "Carbon Vapor Pressure and Heat of Vaporization," Journal of American Chemical Society, 72, 2166 (1950).
17. Van Dyke, M. D.; The Supersonic Blunt Body Problem - Review and Extension, Paper presented at Meeting of the Institute of the Aeronautical Sciences, IAS Preprint No. 801, January 1958.
18. Lees, L.; Hypersonic Flow, Institute of the Aeronautical Sciences Preprint No. 554, 1955, (also California Institute of Technology Publication No. 404).
19. Feldman, S.; Hypersonic Gas Dynamic Charts for Equilibrium Air, Avco Research Laboratory, January 1957.
20. Young, A. D.; College of Aeronautics Report, No. 42 (1951).

APPENDIX A  
TURBULENT CONSERVATION EQUATIONS  
FOR REACTING GAS MIXTURES

The turbulent conservation equations have been studied for compressible flow in references (2) and (20). A similar investigation is carried out here for reacting gas mixtures in a slightly different manner.

The instantaneous value of each of the unknowns is separated into a mean and a fluctuating part such that:

$$Z = \bar{Z} + Z' \quad (A-1)$$

where  $Z$  may be any one or any combination of the physical variables. Introduction of expressions such as equation (A-1) into the full instantaneous conservation equations for reacting gas mixtures and averaging according to the Reynolds rules for time averages yields the following conservation equations which include correlations between fluctuating components:

Continuity for Molecular Species

$$\frac{\partial \bar{\rho} \bar{c}_i}{\partial t} + \nabla \cdot [(\bar{\rho} \bar{c}_i) \bar{u}_i + (\bar{\rho} \bar{c}_i)' u_i' + \bar{\rho} (c_i' \bar{u}_i)] = \bar{w}_i \quad (A-2)$$

where  $\kappa_i$  is the mass fraction,  $\vec{q}_{di}$  the diffusion velocity and  $\omega_i$  is the mass rate of production per unit volume of the  $i$ th species. It is assumed that diffusion due to temperature and pressure gradients is negligible compared to that due to concentration gradients and that all diffusion coefficients are equal. Under these conditions the average of molecular diffusion terms can be expanded to give:

$$\rho(\kappa_i \vec{q}_{di}) = -\bar{\rho} \bar{D} \nabla \bar{\kappa}_i - \bar{\rho}' \bar{D}' \nabla \bar{\kappa}_i - (\bar{\rho} \bar{D}' + \bar{\rho}' \bar{D} + \bar{\rho}' \bar{D}') \nabla \kappa_i' \quad (\text{A-3})$$

where  $D$  is the diffusion coefficient. Two additional continuity equations can be formed from linear sums of equation (A-2).

#### Overall Continuity Equation

$$\frac{\partial \bar{\rho}}{\partial t} + \nabla \cdot (\bar{\rho} \vec{q}) = 0 \quad (\text{A-4})$$

This equation is obtained by summing equation (A-2) over  $i$ .

#### Continuity for Atomic Species

$$\frac{\partial \bar{\rho} \bar{T}_m}{\partial t} + \nabla \cdot [(\bar{\rho} \vec{q}) \bar{T}_m + (\bar{\rho}' \vec{q})' \bar{T}_m + \bar{\rho} \sum_i \alpha_{mi} (\kappa_i \vec{q}_{di})] = 0 \quad (\text{A-5})$$

where

$$\bar{T}_m = \sum_i \alpha_{mi} \kappa_i$$

$\alpha_{mi}$  is the atomic mass fraction of species  $m$  irrespective of molecular configuration and  $\alpha_{mi}$  is the mass of atomic species  $m$  per unit mass of molecular species  $i$ . This equation is obtained by multiplying each expression (A-2) by  $\alpha_{mi}$  and summing over  $i$ . The assumption of equal diffusion coefficients leads to the following expansion for the diffusion terms in equation (A-5):



$$\rho \frac{d}{dt} (\rho \bar{q}_i) = -\bar{\rho} \bar{D} \nabla \bar{T}_m - \bar{\rho}' \bar{D}' \nabla \bar{T}_m - (\bar{\rho} \bar{D}' + \bar{\rho}' \bar{D} + \bar{\rho} \bar{D}') \nabla \bar{T}_m \quad (\text{A-6})$$

### Momentum

$$\frac{\partial \bar{\rho} \bar{q}}{\partial t} + \nabla \cdot [(\bar{\rho} \bar{q}) \bar{q} + (\bar{\rho} \bar{q})' \bar{q}' - \bar{P}] = 0 \quad (\text{A-7})$$

The average stress tensor is in expanded form:

$$\begin{aligned} \bar{P} = & \left\{ - \left( \bar{P} + \frac{2}{3} \bar{\mu} \nabla \cdot \bar{q} \right) \bar{I} + \bar{\mu} \bar{e} \right\} \\ & - \frac{2}{3} \bar{\mu}' \nabla \cdot \bar{q}' \bar{I} + \bar{\mu}' \bar{e}' \end{aligned} \quad (\text{A-8})$$

where  $\bar{\mu}$  is the coefficient of viscosity,  $\bar{I}$  is the unit tensor,  $\bar{e}$  is the rate of strain tensor and  $\bar{P}$  is the pressure.

Energy

$$\begin{aligned}
 \frac{\partial}{\partial t} (\overline{\rho h_s - p}) + \nabla \cdot [ \overline{\rho \vec{q}} (\sum_i \overline{\kappa_i h_i} + \frac{\vec{q}^2}{2}) \\
 + (\overline{\rho \vec{q}})' \{ \sum_i \overline{\kappa_i h_i'} + \overline{\kappa_i' h_i} + \vec{q} \cdot \vec{q}' \} \\
 + \{ \vec{Q} - (\vec{P} \cdot \vec{q} + \overline{P_L} \cdot \vec{q}) \} \\
 + \overline{\rho \vec{q}} (\sum_i \overline{\kappa_i' h_i'} + \frac{\vec{q}'^2}{2}) \\
 + (\overline{\rho \vec{q}})' (\sum_i \overline{\kappa_i' h_i'} + \frac{\vec{q}'^2}{2}) ] = 0
 \end{aligned}
 \tag{A-9}$$

where  $h_s$  is the total enthalpy including chemical enthalpy and kinetic energy,  $h_i$  is the enthalpy of the  $i$ th molecular species including chemical energy, and  $\vec{Q}$  is the flux of heat by conduction and diffusion. The average of molecular dissipation, work and heat transport is given by:

$$\begin{aligned}
& -\overline{\vec{q}} + (\overline{\vec{P} \cdot \vec{q}} + \overline{P \vec{T} \cdot \vec{q}}) = \\
& \left\{ \overline{\kappa \nabla \tau} + \overline{\rho \bar{D}} \sum_i \overline{h_i \nabla h_i} + [\overline{\mu \vec{e}} - \frac{2}{3} \overline{\mu \nabla \cdot \vec{q}} \vec{I}] \cdot \overline{\vec{q}} \right\} \\
& + \left\{ \overline{\kappa' \nabla \tau'} + \overline{\rho' \bar{D}} \sum_i \overline{h_i' \nabla h_i'} + \overline{\rho' D'} \sum_i \overline{h_i \nabla h_i} \right. \\
& \quad + \overline{(\bar{\rho} D' + \rho' \bar{D}) \sum_i [\overline{h_i \nabla h_i'} + \overline{h_i' \nabla h_i}]} \\
& \quad + [\overline{\mu \vec{e}'} + \overline{\mu' \vec{e}} - \frac{2}{3} (\overline{\mu \nabla \cdot \vec{q}'} + \overline{\mu' \nabla \cdot \vec{q}}) \vec{I}] \cdot \overline{\vec{q}'} \\
& \quad \left. + [\overline{\mu' \vec{e}'} - \frac{2}{3} \overline{\mu' \nabla \cdot \vec{q}'} \vec{I}] \cdot \overline{\vec{q}} \right\} \\
& + \left\{ \overline{(\bar{\rho} D' + \rho' \bar{D}) \sum_i h_i' \nabla h_i'} + \overline{\rho' D' \sum_i [\overline{h_i \nabla h_i'} + \overline{h_i' \nabla h_i}]} \right. \\
& \quad \left. + [\overline{\mu' \vec{e}'} - \frac{2}{3} \overline{\mu' \nabla \cdot \vec{q}'} \vec{I}] \cdot \overline{\vec{q}'} \right\} \\
& + \overline{\rho' D' \sum_i h_i' \nabla h_i'}
\end{aligned}$$

(A-10)

Equation of State

$$\bar{P} = \frac{\overline{\rho R_0 T}}{M} \quad (A-11)$$

where

$$\frac{1}{M} = \sum_i \frac{\pi_i}{M_i}$$

In each conservation relation given by equations (A-2), (A-5), (A-7) and (A-9) the first term inside the brackets represents the influence of convection, while the second term represents transport of properties by turbulent motion. In the case of the momentum equation this latter term represents the Reynolds stress tensor.

The third terms which involve averages of molecular transport quantities have been expanded in equations (A-3), (A-6), (A-8) and (A-10). In each of these equations the first terms or group of terms do not involve any fluctuating components. Near a body surface in the laminar sublayer where all fluctuations are damped out due to the influence of the surface and property gradients are large, these first terms are dominant ones. In the fully turbulent region, however, the turbulent transport terms overshadow all components of molecular transport. Presumably, in this region the various components of the average molecular transport terms which involve correlations between fluctuating transport properties or fluctuating gradients and other fluctuating quantities will be no larger in magnitude than the largest component of the corresponding term involving only average transport properties and gradients in equations (A-3), (A-6), (A-8), and (A-10). Since it is to be expected that all components of the turbulent transport terms are about the same magnitude each component involving correlations between molecular transport fluctuations will be overshadowed by the turbulent transport terms in the fully turbulent region. Presumably, corresponding derivatives behave the same way. Therefore, it should be necessary to retain only the first term or group of terms in the expansions given by equations (A-3), (A-6), (A-8) and (A-10), except possibly in the buffer layer between the sublayer and the fully turbulent

region. No attempt will be made to account for this latter complication in the buffer layer. The last term in the energy equation is a triple correlation and should be small compared to double correlations. In addition, it is assumed that  $(\sum \kappa_i' h_i' + \frac{q_i'^2}{2}) \ll (\sum \kappa_i' h_i' + \frac{q_i'^2}{2})$ .

In the mean steady state, then, only the first two terms in bracket of the conservation equations plus the first terms of the expansions are retained. The equations are now prepared for introduction of the usual boundary layer assumptions which lead to the equations of Section 2.

## APPENDIX B

### DISCUSSION OF THE NUMBER OF INDEPENDENT RELATIONS FOR MOLECULAR SPECIES

Although it may be intuitively obvious that the atomic mass fractions,  $T_m$ , plus the rates of reaction,  $W_i$ , are sufficient to determine all of the molecular mass fractions,  $\pi_i$ , it is of interest to show this in a formal way and also to show how many of these quantities are required. Suppose it is assumed that the system contains  $P$  molecular compounds formed by reactions between air and the surface material and that these molecular species are built from  $S$  atomic species. Then the atomic mass fractions are given by:

$$\frac{T_m}{M_m} = \sum_{i=1}^P \alpha_{mi} \left( \frac{\pi_i}{M_i} \right) \quad m = 1, 2, \dots, S \quad (B-1)$$

where  $\alpha_{mi}$  is the number of atoms of atomic species  $m$  contained in molecular species  $i$  and may be zero. From the theory of linear equations it is known that if the rank of the matrix of  $\alpha_{mi}$  is  $N$  then equation (B-1) represents  $N$  independent equations for the  $P$  molecular mass fractions  $\pi_i$ . In order for equation (B-1) to have any solutions at all it is required that there be  $(S-N)$  relations among the  $S$  atomic mass fractions  $T_m$  which can be obtained by making the  $T_m$ 's orthogonal to the solutions, if any, of the homogeneous equation formed with the transposed matrix. These relations eliminate any superfluous equations from the system. In addition, it can be shown that the rates of reaction,  $W_i$ , satisfy:

$$\sum_{i=1}^P \alpha_{i\ell} \left( \frac{w_i}{M_i} \right) = 0 \quad \ell = 1, 2, \dots, S \quad (B-2)$$

Equation (B-2) has  $(P-\mathcal{L})$  independent solutions so that if  $(\mathcal{L})$  of the  $w_i$ 's are known the rest can be determined. These  $(P)$  production rates are related in a nonlinear way to the molecular mass fractions through the law of mass action:

$$w_i = M_i \sum_{\ell=1}^{\mathcal{L}} (v_{i\ell}' - v_{i\ell}'') \left[ k_{\ell} \prod_{j=1}^P \left( \frac{pK_j}{M_j} \right)^{v_{j\ell}'} - k_{\ell}'' \prod_{j=1}^P \left( \frac{pK_j}{M_j} \right)^{v_{j\ell}''} \right] \quad (B-3)$$

$i = 1, 2, \dots, P$

The products are taken over all species which enter into a given reaction,  $\ell$ , while the sums are taken over all of the  $\mathcal{L}$  reactions which occur. The quantities  $k_{\ell}$  and  $k_{\ell}''$  are the forward and backward rate coefficients, respectively. The  $(P-\mathcal{L})$  independent equations (B-3) plus the  $\mathcal{L}$  independent equations (B-1) represent a total of  $P$  equations for the  $P$  unknowns  $pK_i$ . It is assumed that among the roots to this nonlinear set of equations there is one real root for each  $pK_i$  between zero and unity.

In addition to the information already obtained, it is possible to determine how many reactions can occur between the chosen set of molecules and to find a set of reactions which can be regrouped to express the actual reactions. The molecular weight of molecular species  $i$  can be obtained by summing the weights of all atomic species which it contains:

$$M_i = \sum_{m=1}^S \alpha_{im} M_m \quad i = 1, 2, \dots, P \quad (B-4)$$

Since  $\alpha_{im}$  is just the transposed matrix of  $\alpha_{mi}$ , it is also of rank  $r$ . Therefore, in order for the set of equations (B-4) to be consistent it is necessary that the  $M_i$ 's satisfy  $(P-r)$  relationships obtained in a manner similar to that described for the  $T_m$ 's. These  $(P-r)$  relations among the molecular weights can be rearranged to give the actual reactions themselves:

$$\sum_{i=1}^P (v_{i\ell}'' - v_{i\ell}') M_i = 0 \quad \ell = 1, 2, \dots, (P-r) \quad (B-5)$$



## APPENDIX C

### ESTIMATION OF COMBUSTION ZONE THICKNESS

An estimate of the thickness of the combustion zone can be obtained in the following manner. Let:

$$\frac{1}{\Delta \xi_f} = \left( \frac{1}{\kappa_f} \frac{d\kappa_f}{d\xi} \right)_{\xi=\xi^*} \quad (C-1)$$

$$\frac{1}{\Delta \xi_o} = - \left[ \frac{1}{(\kappa_o + \kappa_{o_2})} \frac{d}{d\xi} (\kappa_o + \kappa_{o_2}) \right]_{\xi=\xi^*} \quad (C-2)$$

Differentiation of equation (54) with respect to  $\xi$  then leads to the following expression:

$$\left( \frac{\Delta \xi_f \Delta \xi_o}{\Delta \xi_o + \Delta \xi_f} \right) = \frac{(\kappa_f)_{\xi=\xi^*}}{1 + B^*} \quad (C-3)$$

From the definition of  $\xi$  given by equation (53), the change in velocity ratio is related to the change in  $\xi$  through:

$$|\Delta z| = \frac{1+B}{B} |\Delta \xi| \quad (C-4)$$

If  $\Delta \xi_+$  and  $\Delta \xi_0$  are the same order of magnitude it seems reasonable to define a characteristic change in velocity ratio by means of:

$$\Delta z^* = 2 \frac{(1+B)}{B} \frac{(\kappa_+)_\xi=\xi^*}{1+B^*} \quad (C-5)$$

As discussed in Section 4  $\kappa_+$  is often very small at the combustion zone. Under these conditions the velocity change across the combustion zone is very small. In the fully turbulent region of the boundary layer, however, the velocity changes very slowly with distance from the surface so that in the turbulent region the combustion zone may appear rather thick even when the velocity change is small. In the sublayer where the velocity changes extremely rapidly the zone must appear thin. When  $(\kappa_+)_\xi=\xi^*$  is small the boundary layer is rather sharply divided into two separate regions. On one side of the combustion zone oxygen is mixed with products and inerts while on the other side gaseous fuel is mixed with products and inerts. Since  $(\kappa_+)_\xi=\xi^*$  depends on  $\xi^*$ , temperature and pressure the thickness of the combustion zone can be estimated as a function of  $B$ , temperature, and pressure at the combustion zone for any particular chemical system.

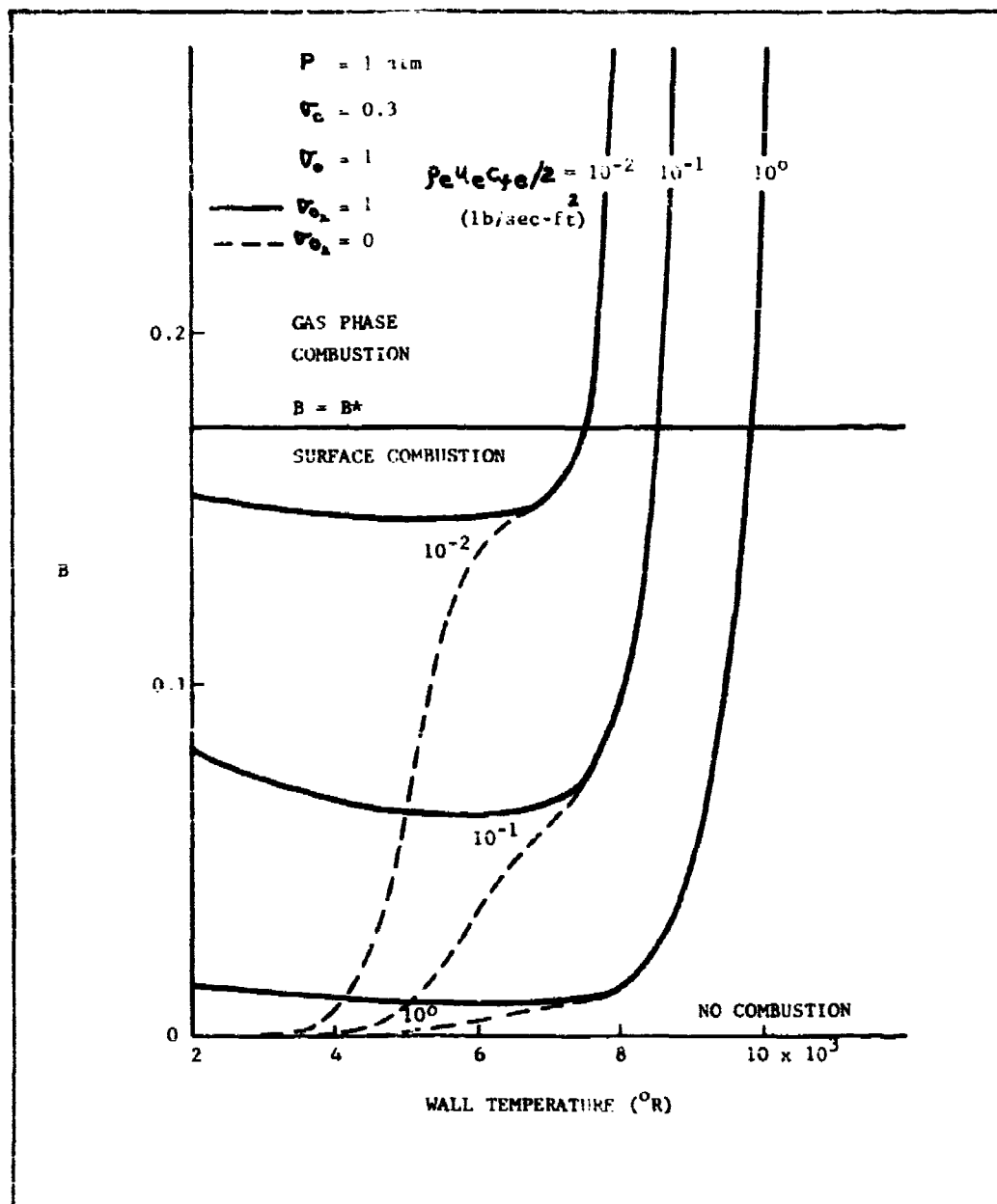


FIG. 1 EFFECT OF FLOW PARAMETER, ACCOMMODATION COEFFICIENT, AND TEMPERATURE ON B

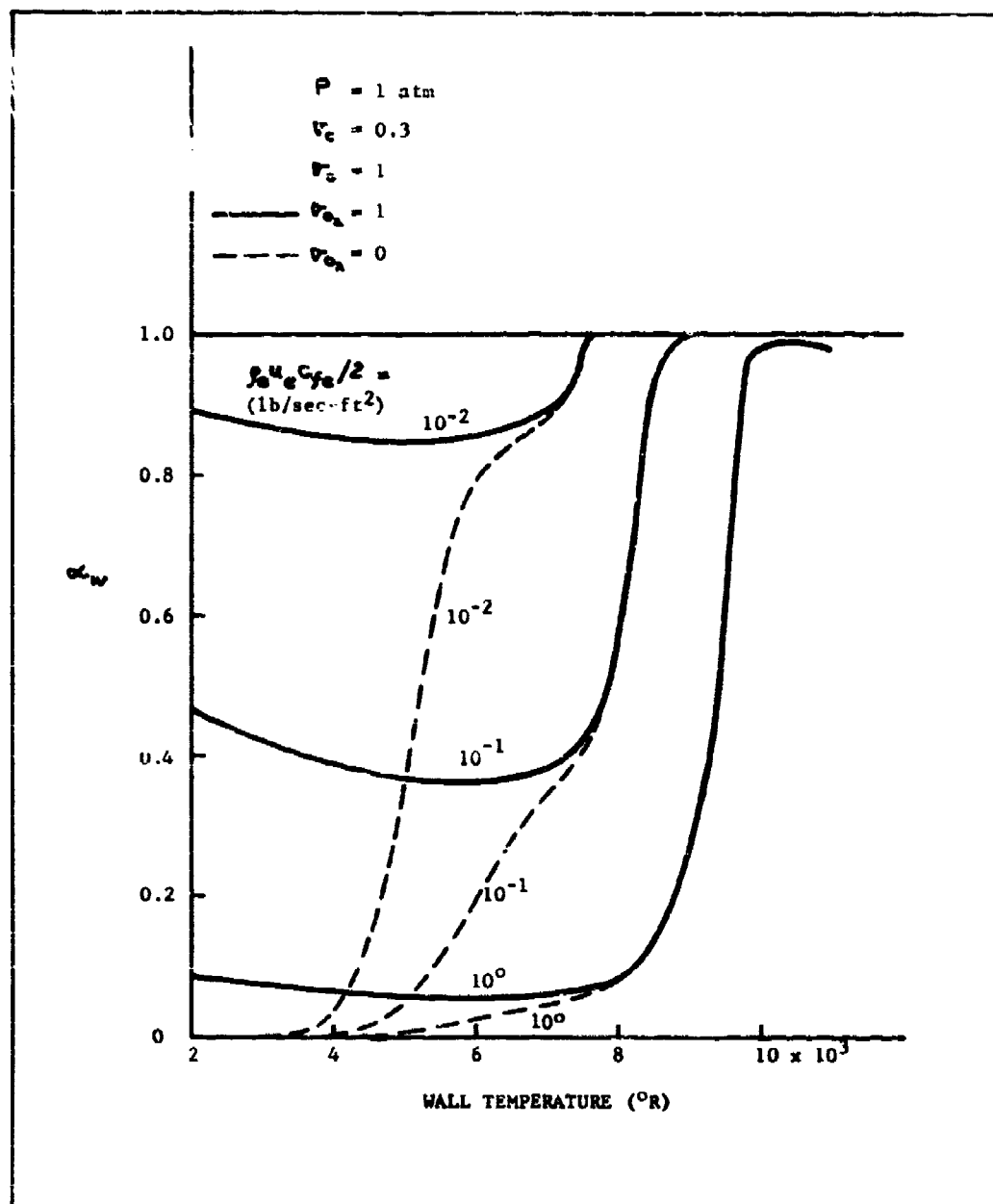


FIG. 2 EFFECT OF FLOW PARAMETER, ACCOMMODATION COEFFICIENT, AND TEMPERATURE ON  $\alpha_w$

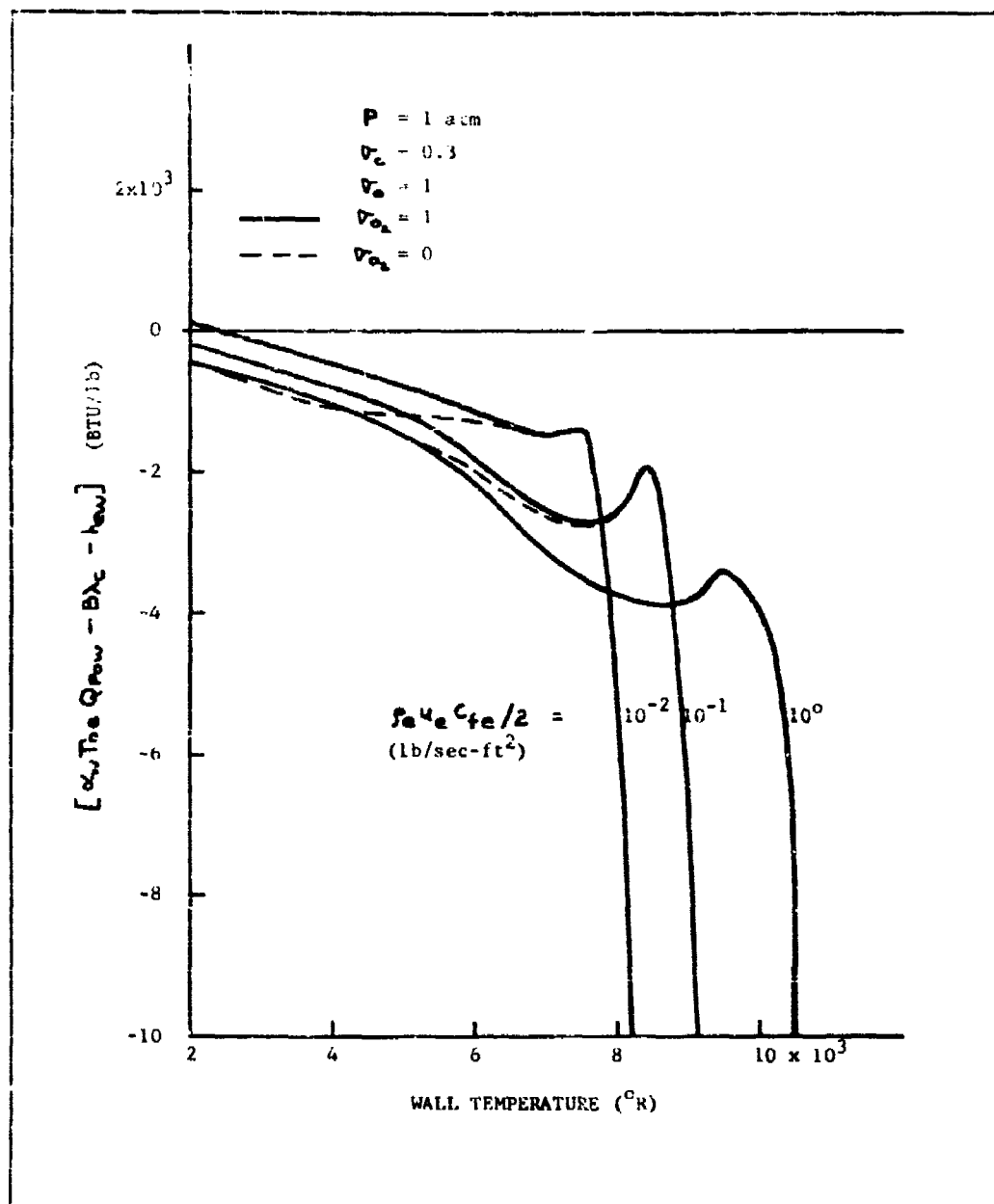


FIG. 3 EFFECT OF FLOW PARAMETER, ACCOMMODATION COEFFICIENT, AND TEMPERATURE ON ENTHALPY POTENTIAL

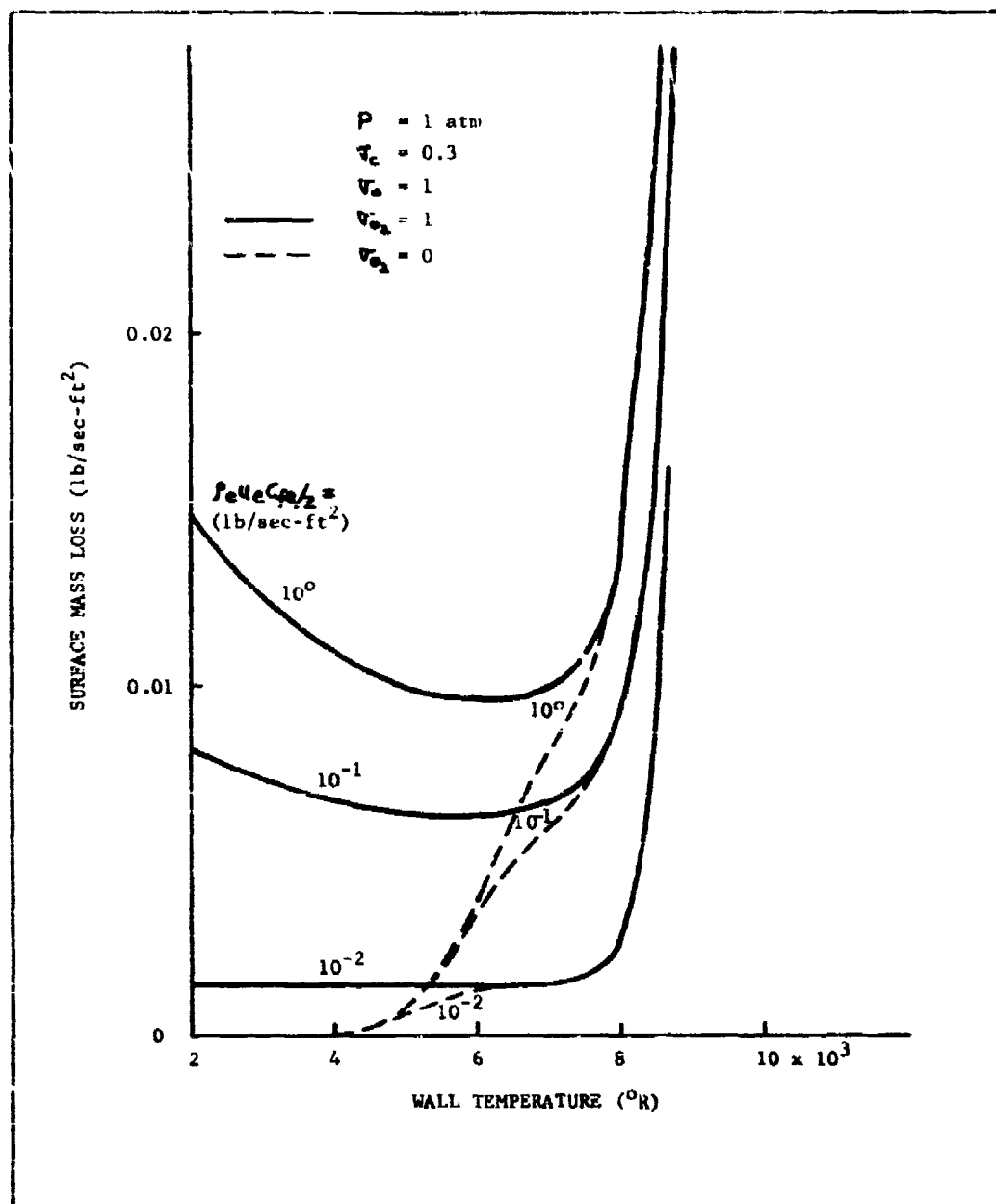


FIG. 4 EFFECT OF FLOW PARAMETER, ACCOMMODATION COEFFICIENT, AND TEMPERATURE ON SURFACE MASS LOSS

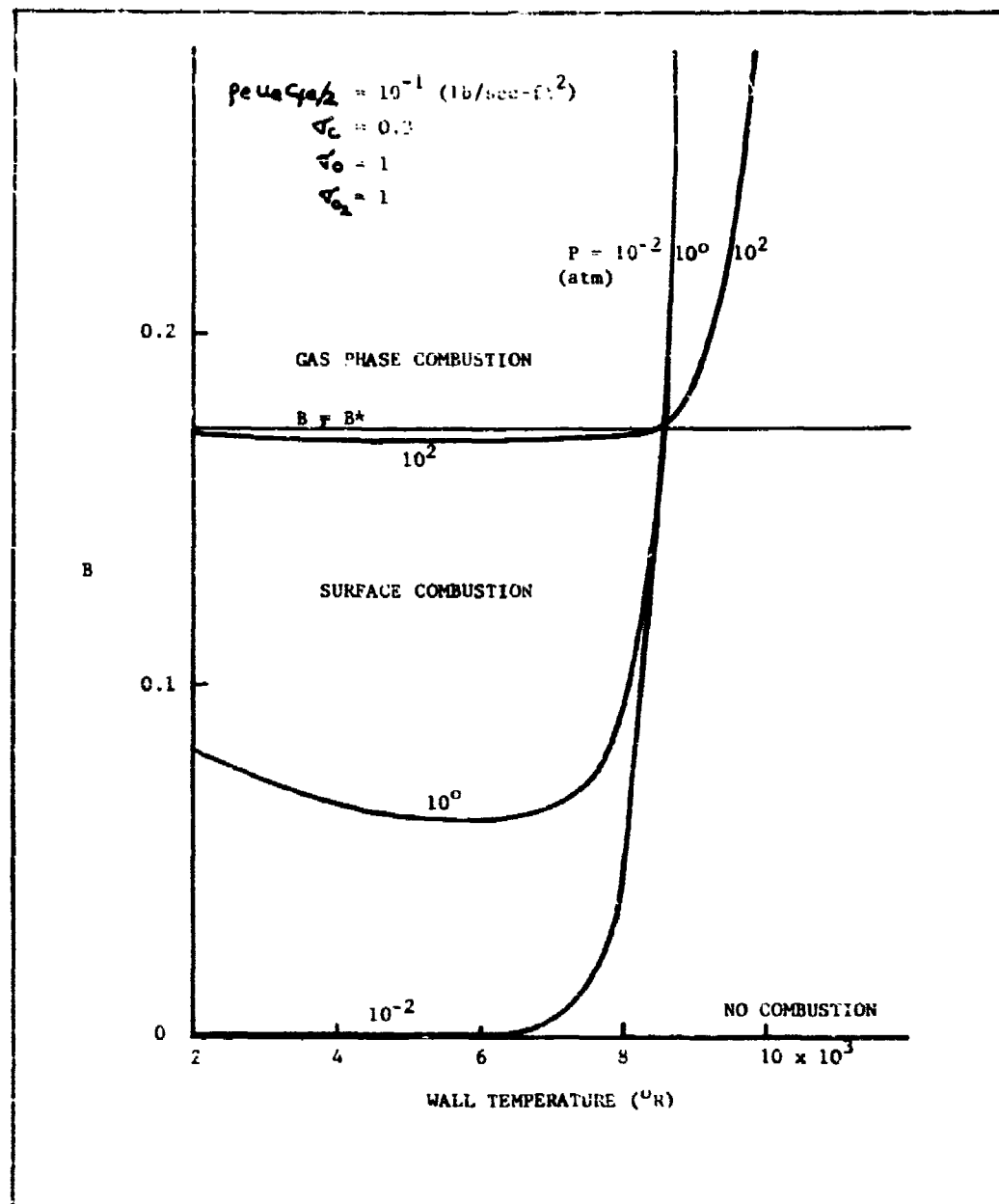


FIG. 5 EFFECT OF PRESSURE AND TEMPERATURE ON B

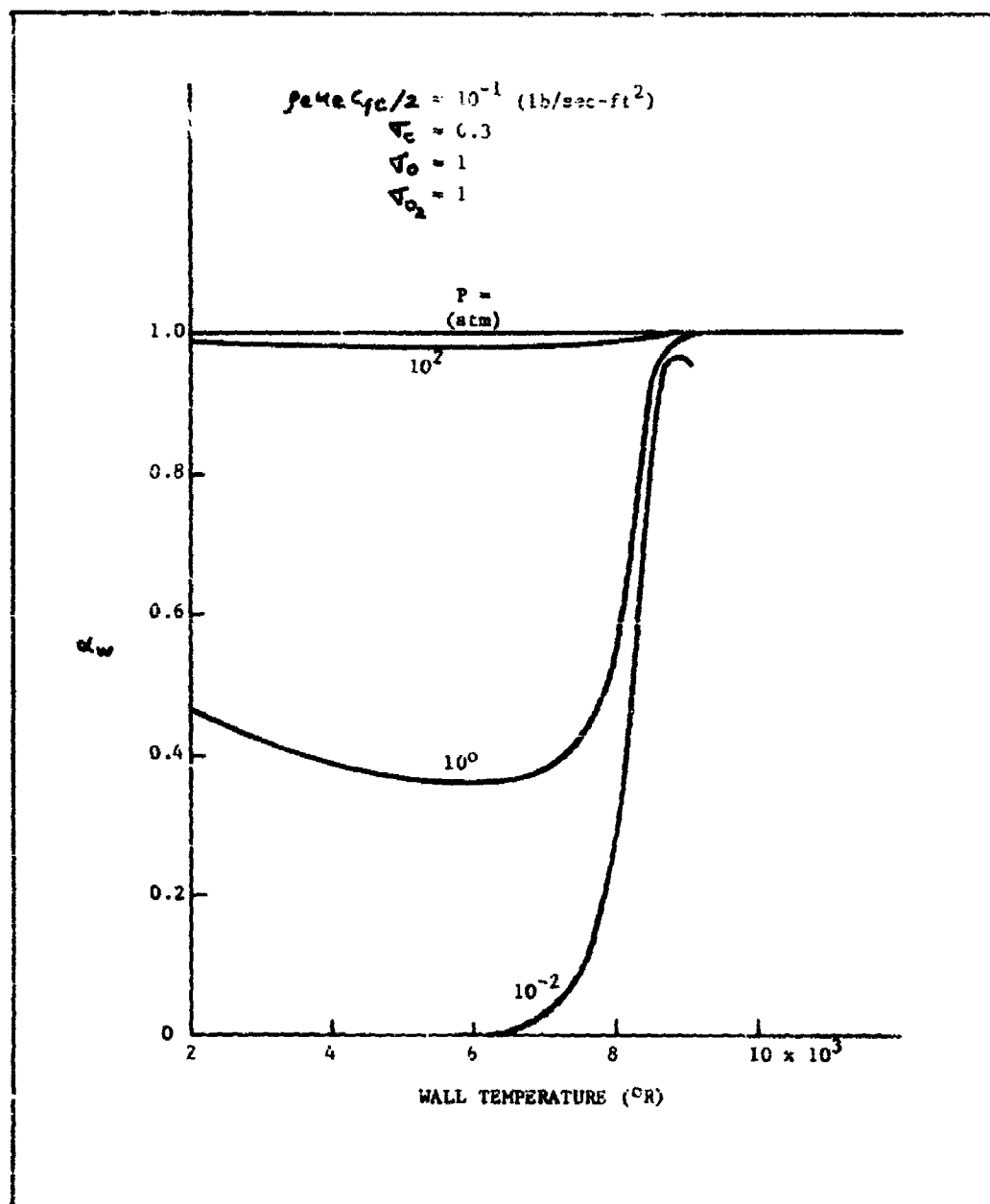


FIG. 6 EFFECT OF PRESSURE AND TEMPERATURE ON  $\alpha_w$



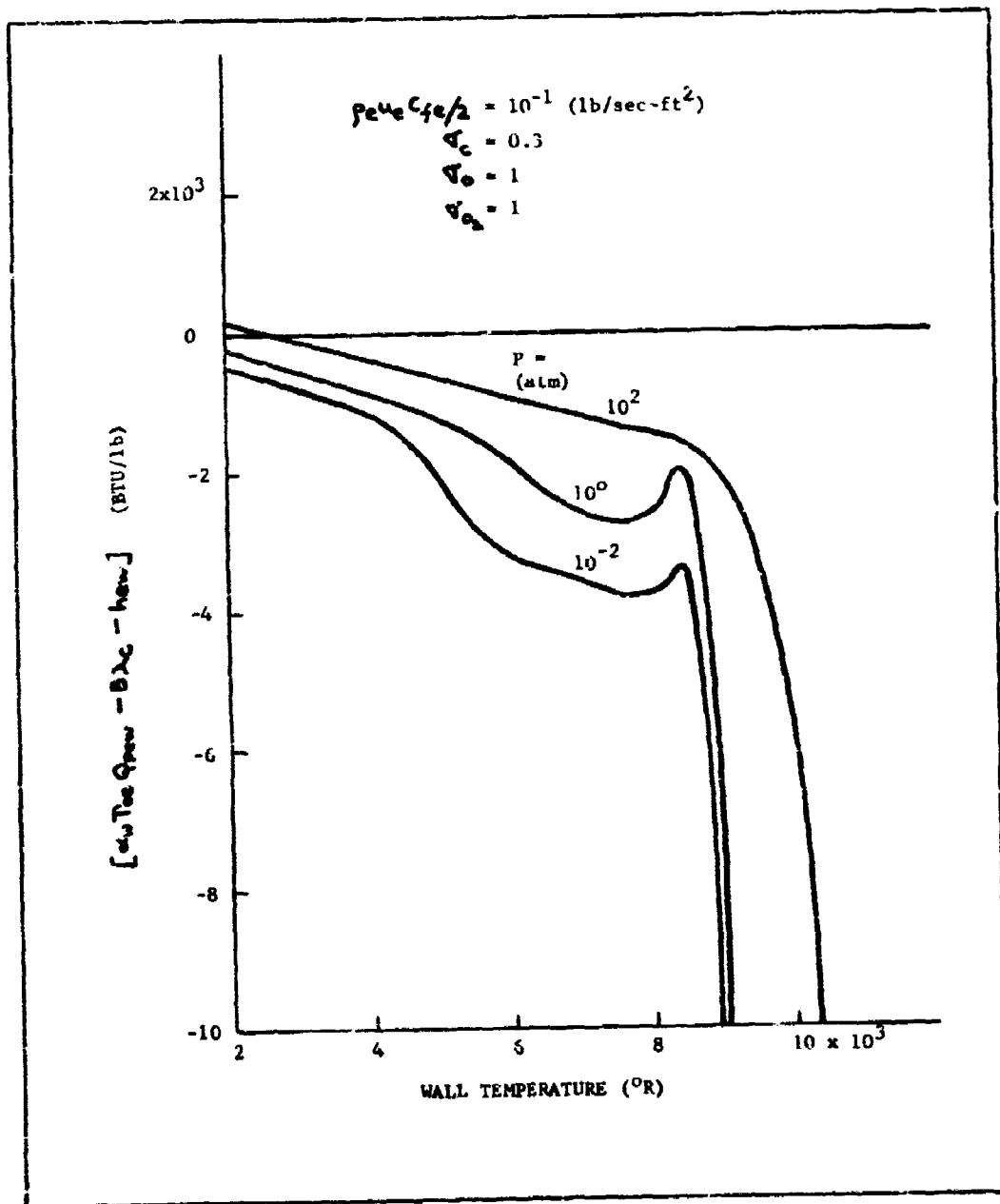


FIG. 7 EFFECT OF PRESSURE AND TEMPERATURE ON ENTHALPY POTENTIAL

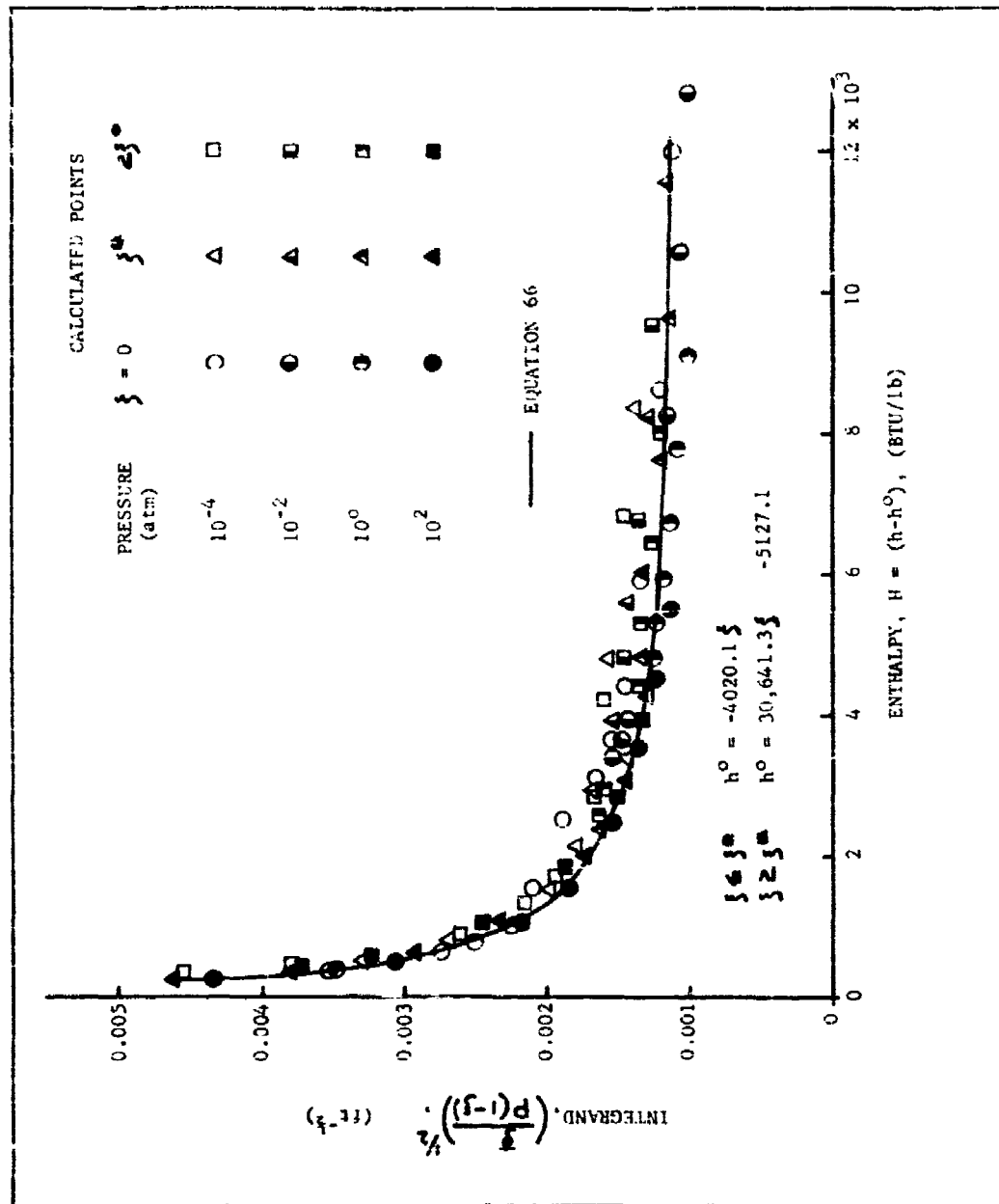


FIG. 8 UNIVERSAL PLOT FOR INTEGRAND OF  $\phi$   
(GRAPHITE IN AIR)

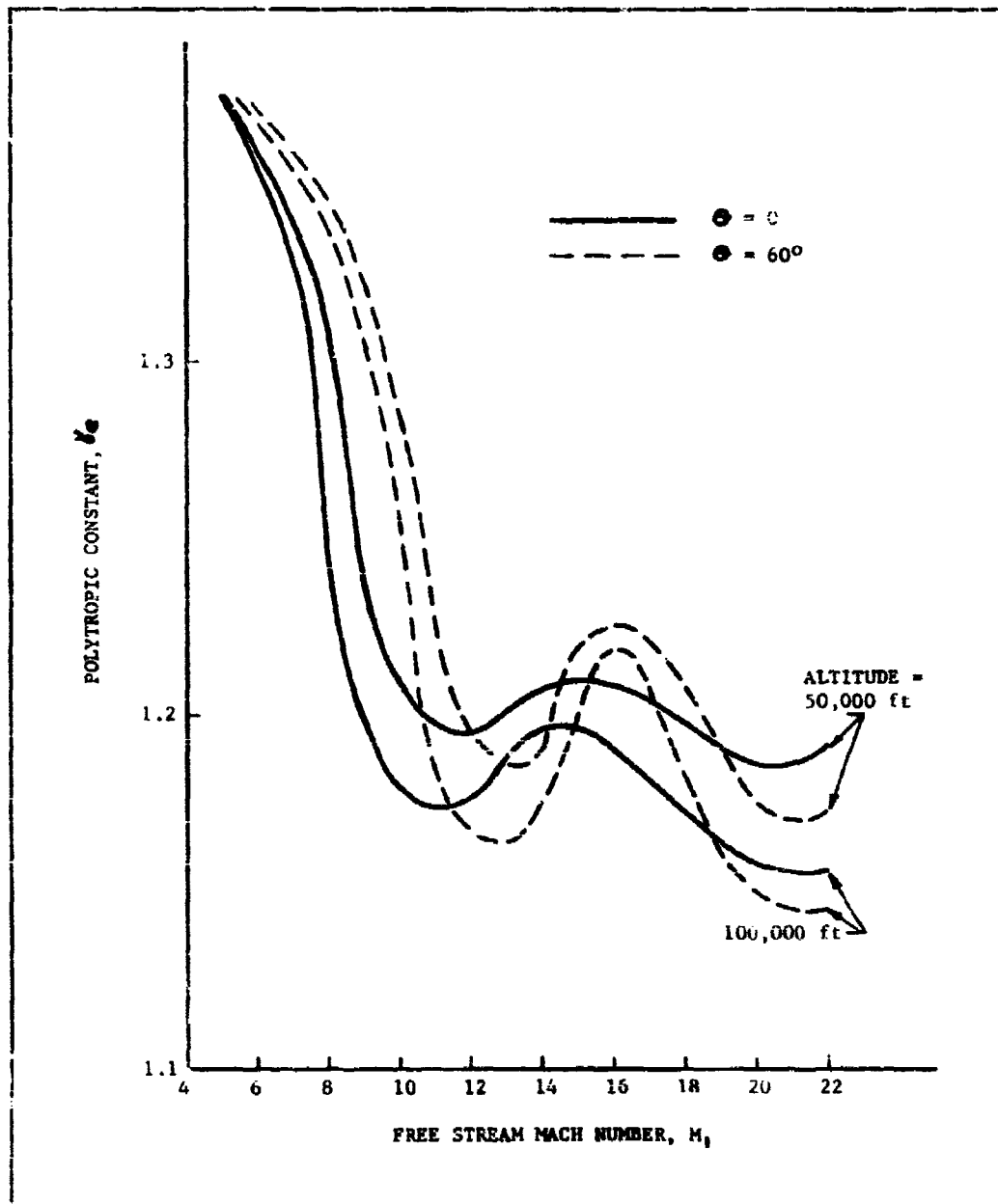


FIG. 9 VARIATION OF  $k_e$  WITH MACH NUMBER, ALTITUDE AND ANGULAR LOCATION ON A HEMISPHERE

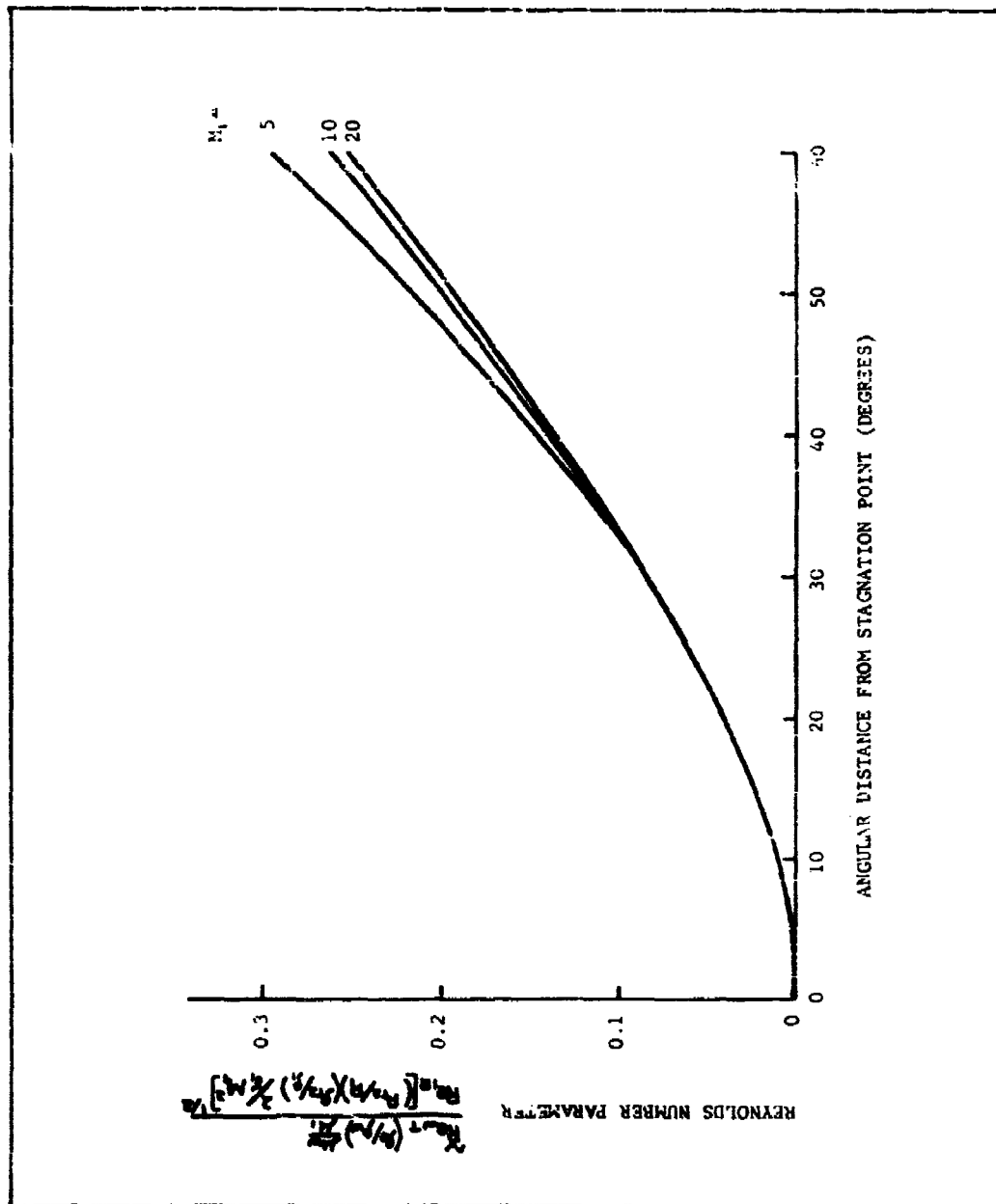


FIG. 10 EFFECTIVE REYNOLDS NUMBER PARAMETER FOR A HEMISPHERE

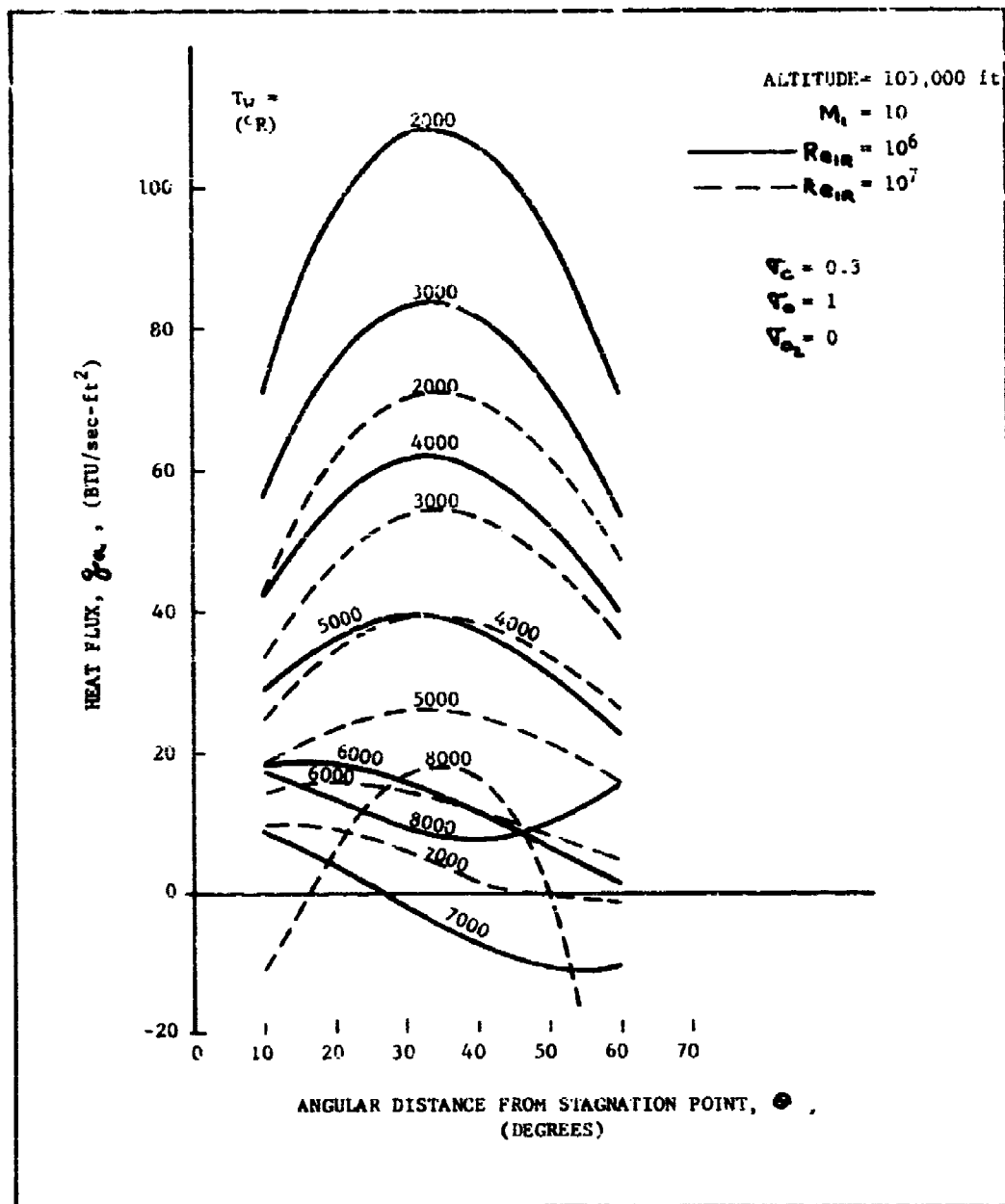


FIG. 11 HEAT FLUX DISTRIBUTION ON HEMISPHERE--  
100,000 FT ALTITUDE

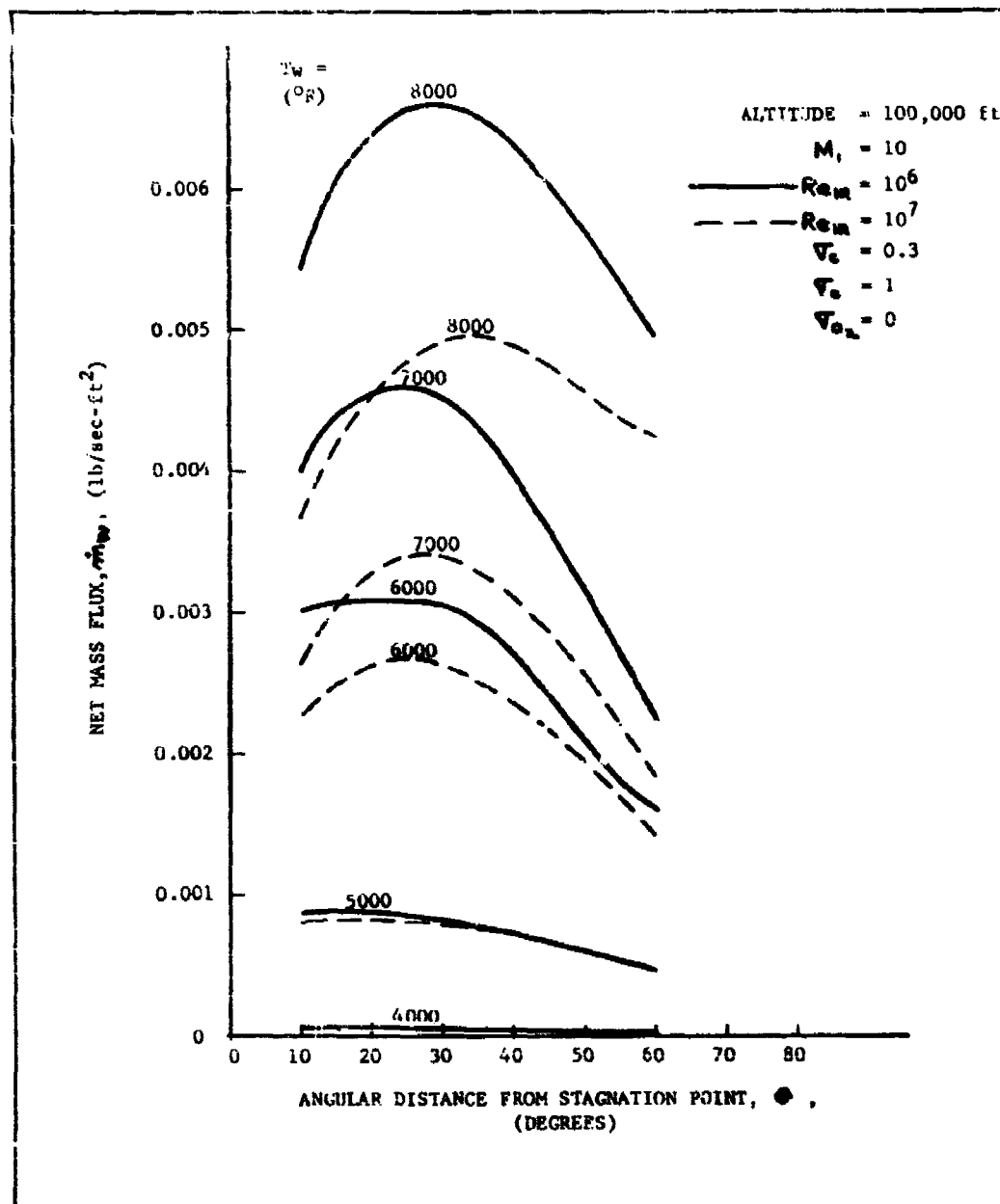


FIG. 12 MASS FLUX DISTRIBUTION ON HEMISPHERE--  
 100,000 FT ALTITUDE

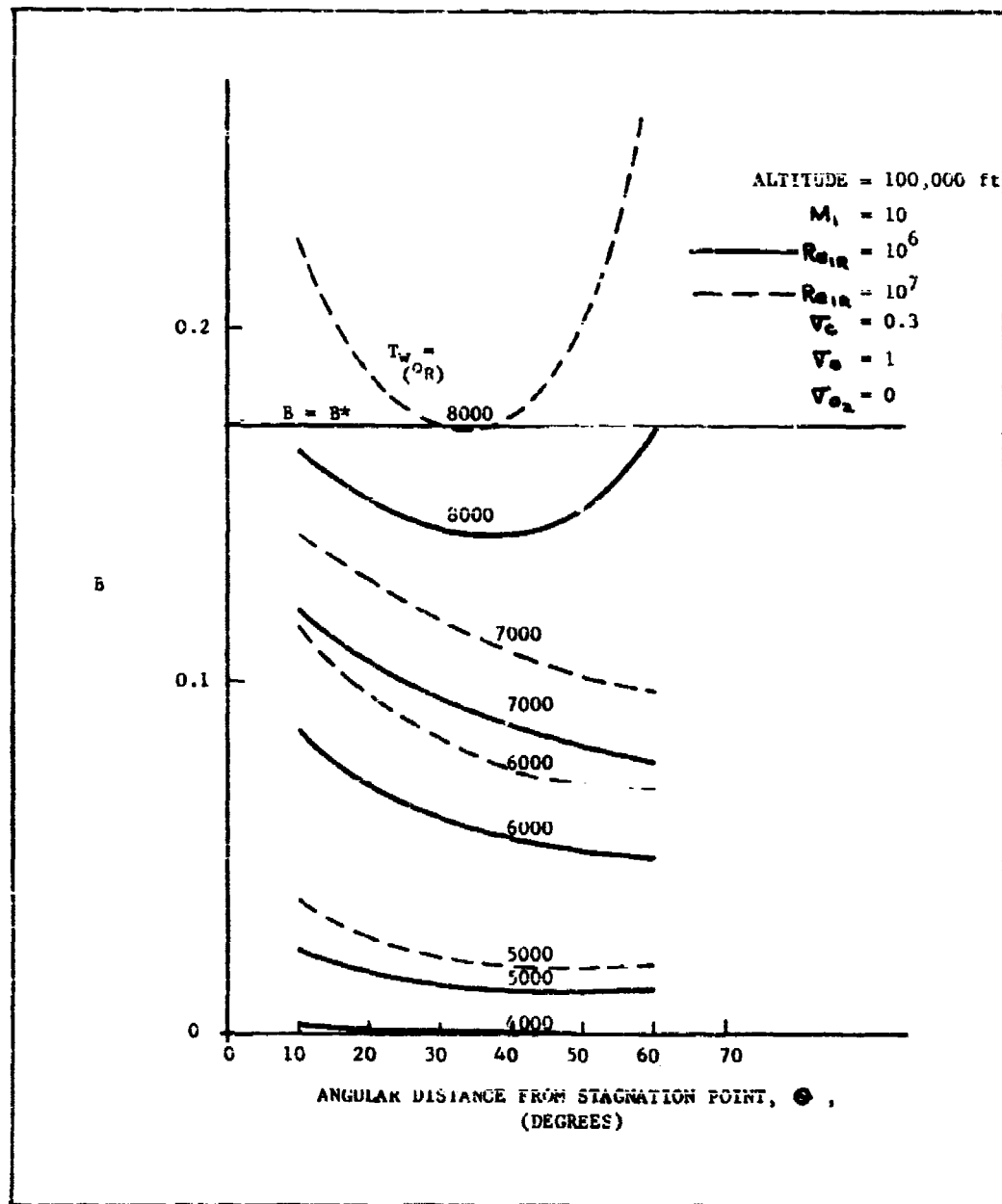


FIG. 13 DISTRIBUTION OF PARAMETER B ON HEMISPHERE--  
100,000 FT ALTITUDE

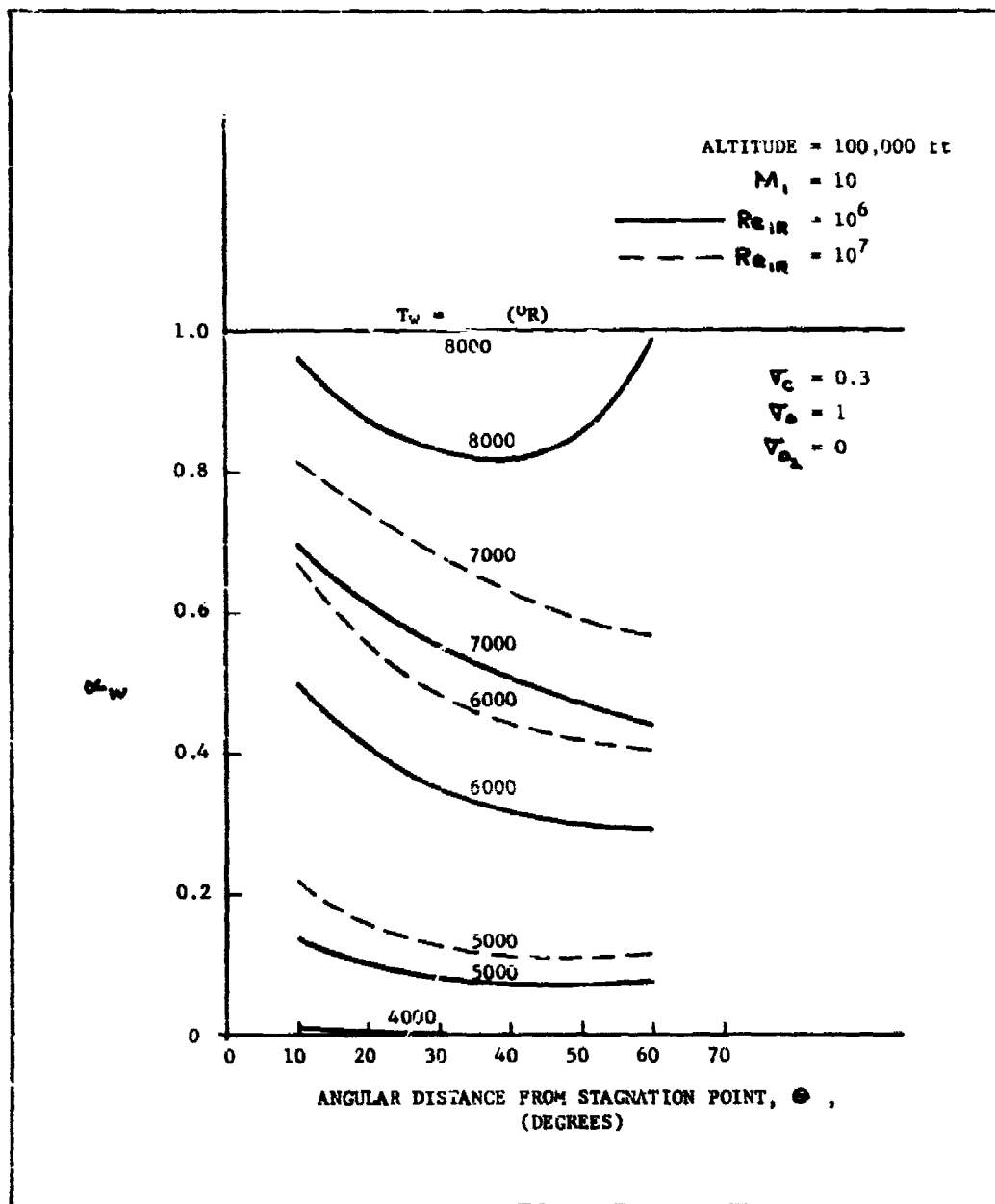


FIG. 14 DISTRIBUTION OF PARAMETER  $\alpha_w$  ON HEMISPHERE--  
100,000 FT ALTITUDE



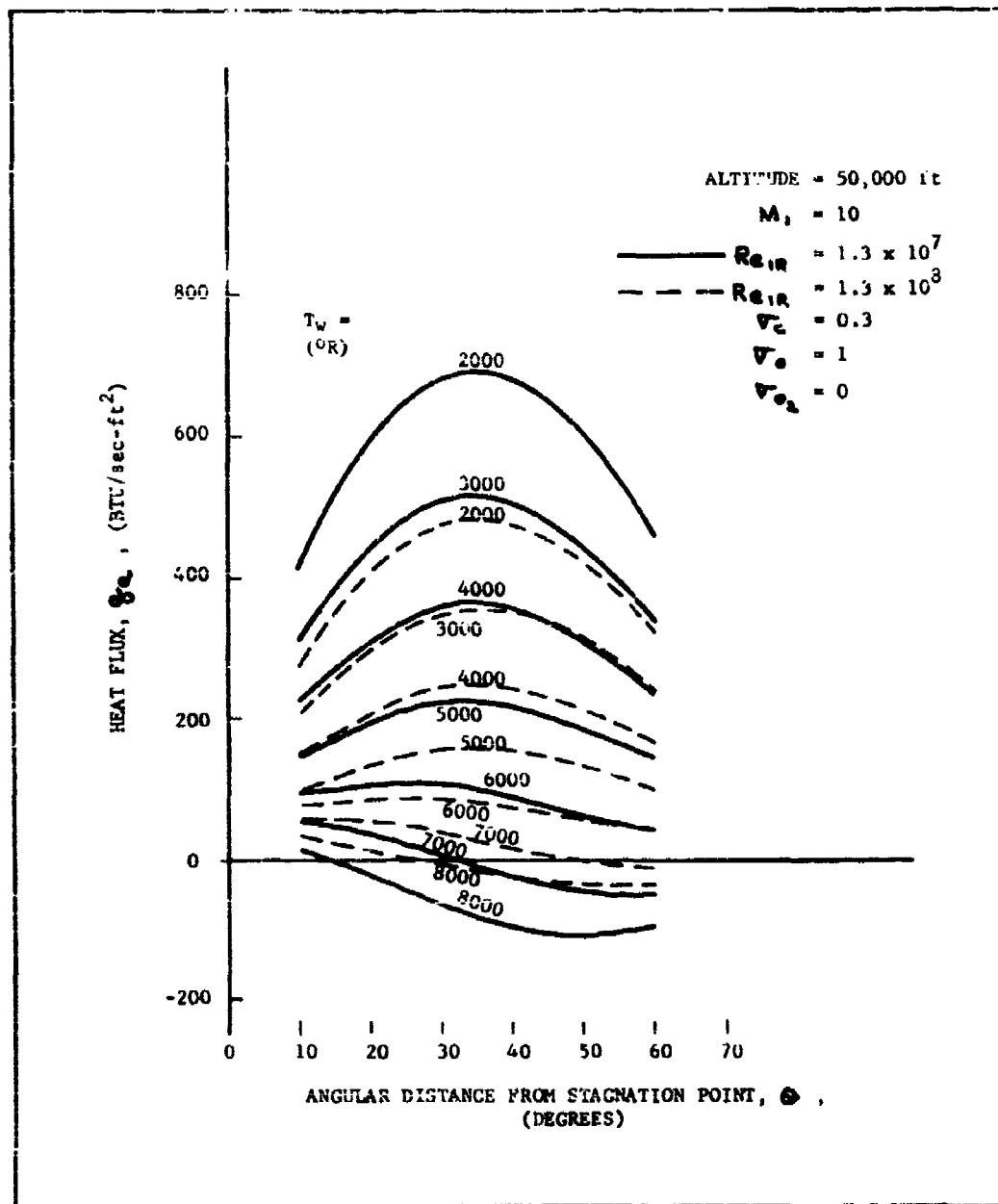


FIG. 15 HEAT FLUX DISTRIBUTION ON HEMISPHERE--  
50,000 FT ALTITUDE

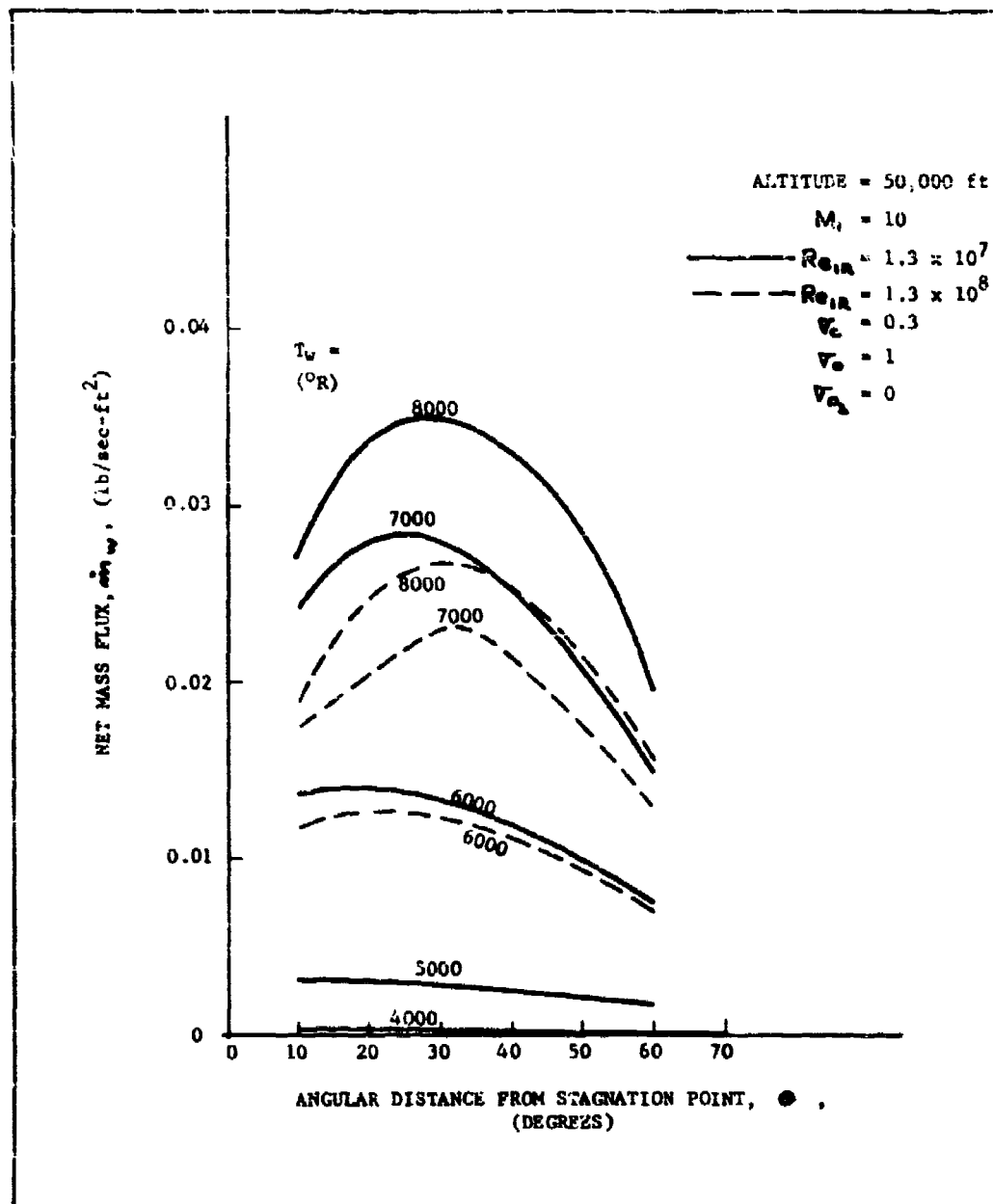


FIG. 16 MASS FLUX DISTRIBUTION ON HEMISPHERE--  
50,000 FT ALTITUDE

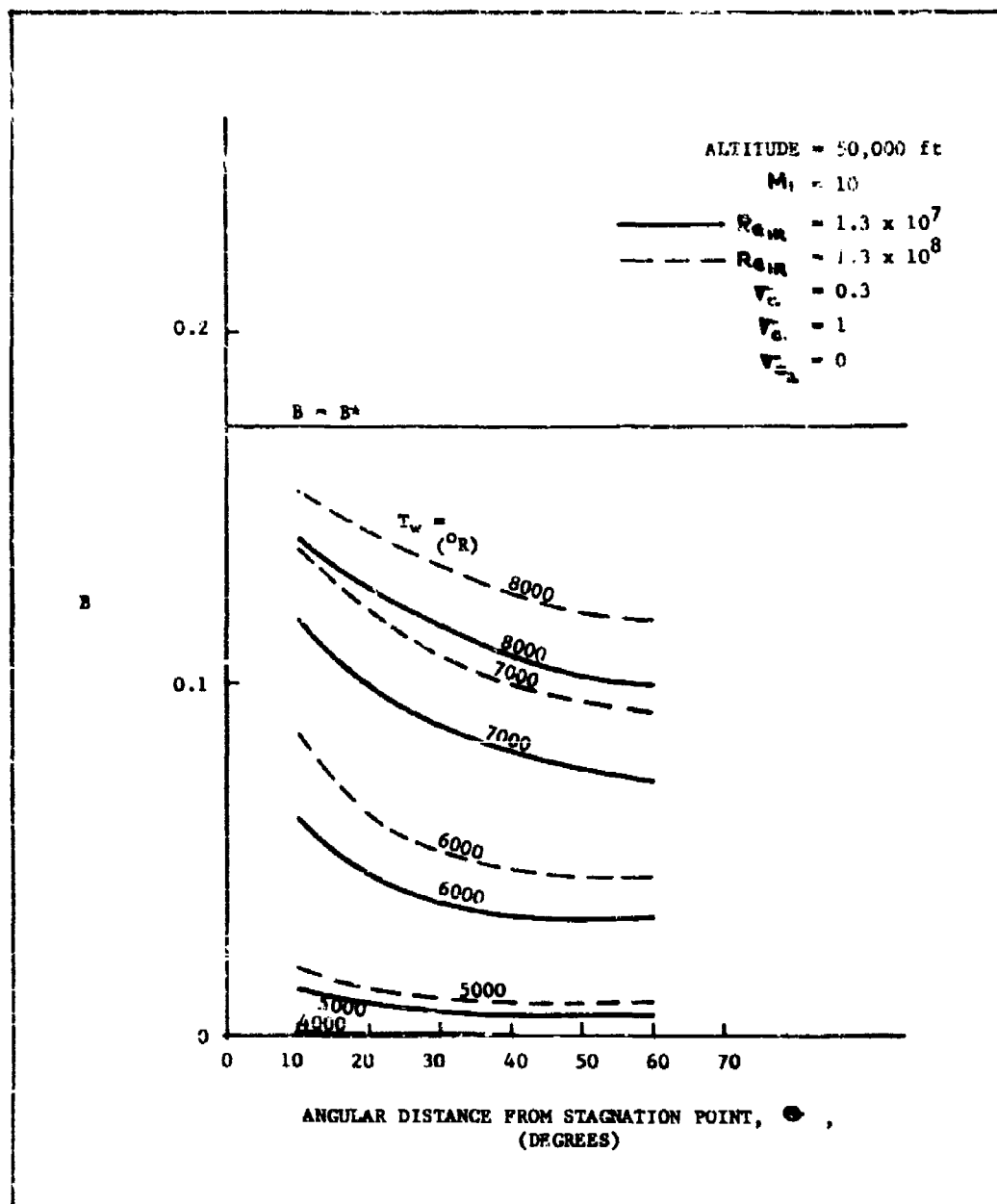


FIG. 17 DISTRIBUTION OF PARAMETER B ON HEMISPHERE--  
50,000 FT ALTITUDE

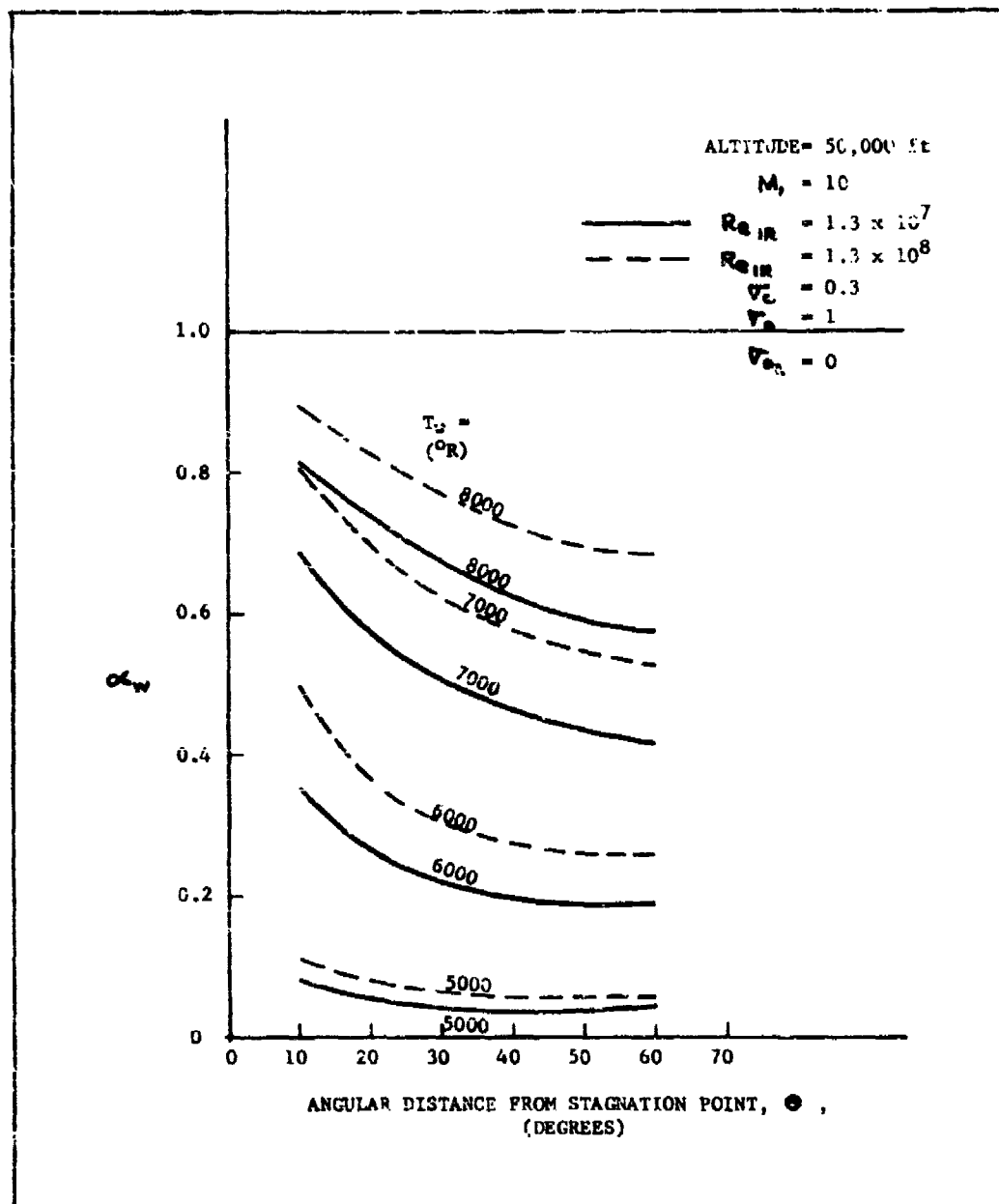


FIG. 18 DISTRIBUTION OF PARAMETER  $\alpha_w$  ON HEMISPHERE--  
50,000 FT ALTITUDE

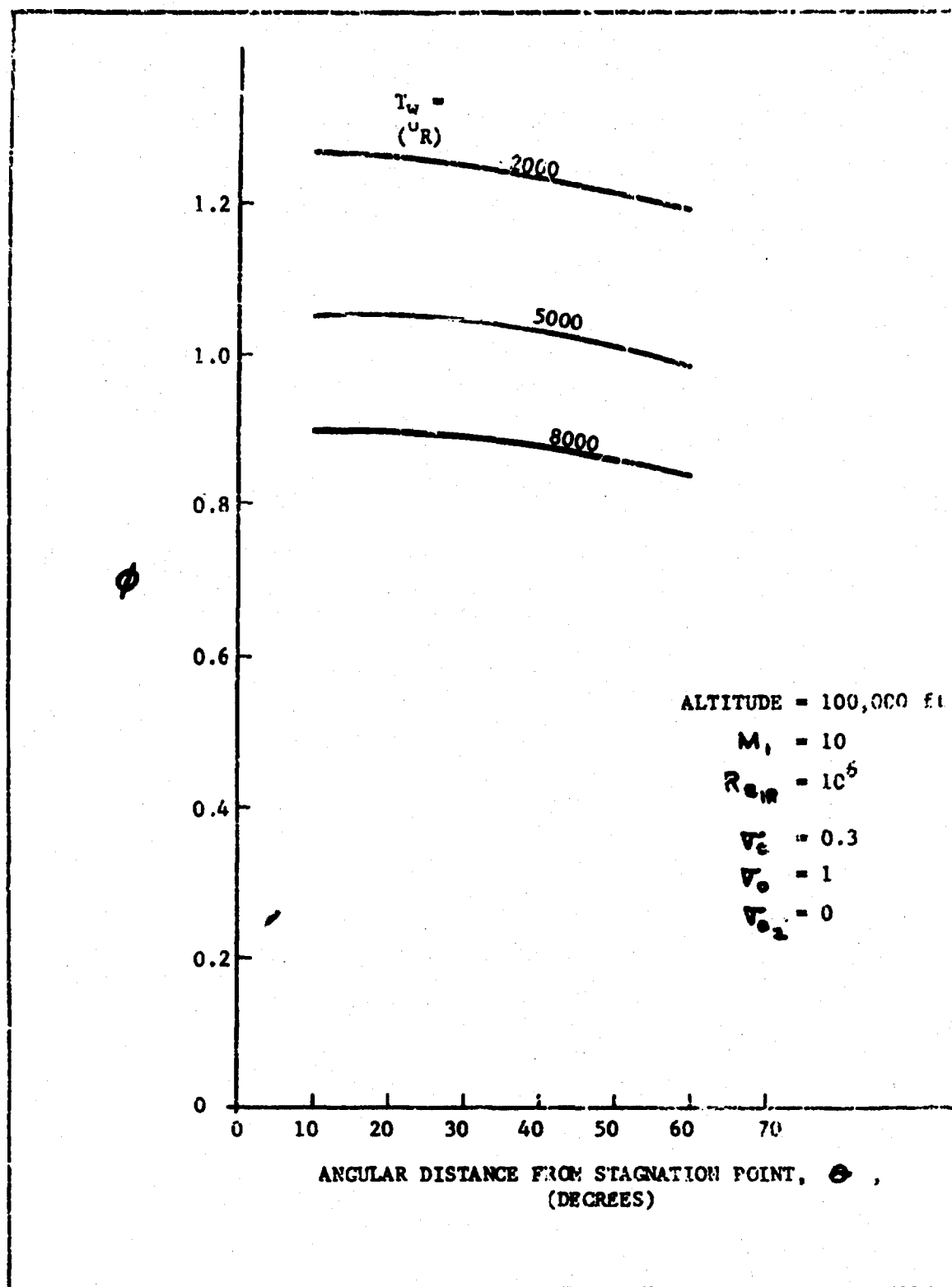


FIG. 19 DISTRIBUTION OF INTEGRAL  $\phi$  ON HEMISPHERE